Електромагнитни взаимодействия и структура на ядрата и елементарните частици

QED като калибровъчна теория

- Свободен Дираков фермион: $\mathcal{L} = \bar{\psi}\,(i\gamma^{\mu}\partial_{\mu} - m)\,\psi$
- Фазова инвариантност: $\psi \to \psi' = e^{iQ\theta}\psi \quad ; \quad \bar{\psi} \to \bar{\psi}' = e^{-iQ\theta}\,\bar{\psi}$

Абсолютните стойности на фазите са ненаблюдаеми в квантовата механика. Лагранжиянът е инвариантен относно фазово преобразуване.

- **КАЛИБРОВЪЧЕН ПРИНЦИП:** $\theta = \theta(x)$

Ако фазовата инвариантност е **ЛОКАЛНА** то

$$\partial_{\mu}\psi \to e^{iQ\theta}\,(\partial_{\mu} + i\,Q\,\partial_{\mu}\theta)\,\psi$$

Лагранжиянът вече не е инвариантен относно фазово преобразуване.

Въвеждаме ковариантни производни $D_{\mu}\psi \equiv (\partial_{\mu} + i\,e\,Q\,A_{\mu})\,\psi$

като $A_{\mu} \to A_{\mu} - \frac{1}{e}\,\partial_{\mu}\theta$

Файнманови диаграми

The Basic Building Blocks

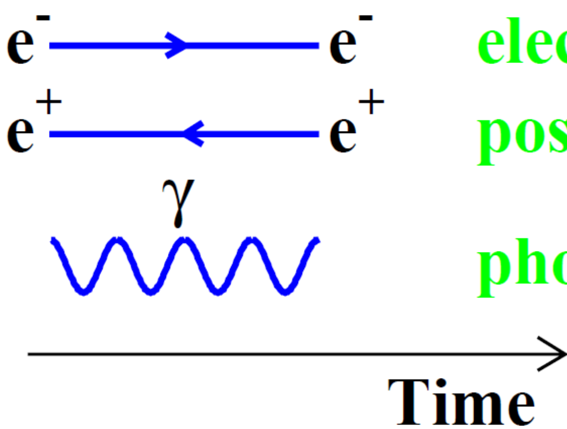

electron

positron

photon

Note : the positron (e^+) line is drawn as a negative energy electron traveling backwards in time

The $e^{\pm}$ – photon interactions

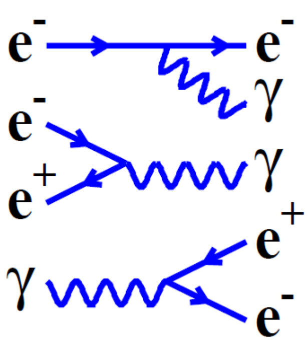

Radiation

Annihilation

Pair Prod.

Note: none of these processes are allowed in isolation : Forbidden by $(E, \tilde{\mathrm{p}})$ conservation.

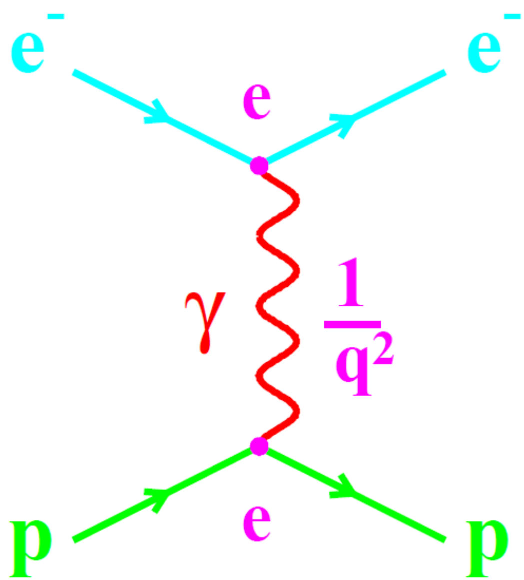

Electron Current

Propagator

Proton Current

Matrix element M factorises into 3 terms :

$$
\begin{aligned}
-iM &= \langle \overline{u}_e | ie\gamma^\mu | u_e \rangle \quad \text{Electron Current} \\
&\times \frac{-ig^{\mu\nu}}{q^2} \quad \text{Photon Propagator} \\
&\times \langle \overline{u}_p | ie\gamma^\nu | u_p \rangle \quad \text{Proton Current}
\end{aligned}
$$

Compton Scattering

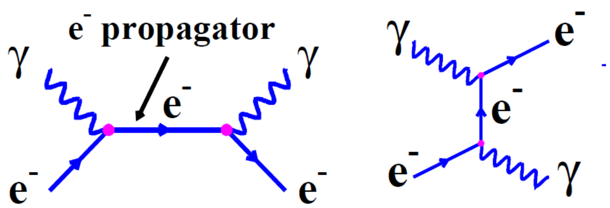

$$\sigma \sim |M|^2 \sim e^4$$

Bremsstrahlung

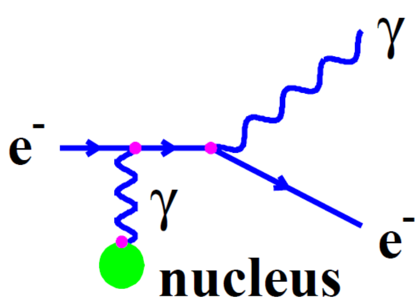

$$|M|^2 \sim Z^2 e^6$$

e^+e^- Pair Production

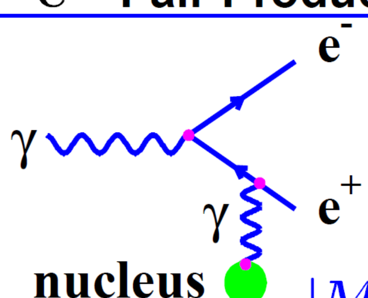

$$|M|^2 \sim Z^2 e^6$$

ep Scattering

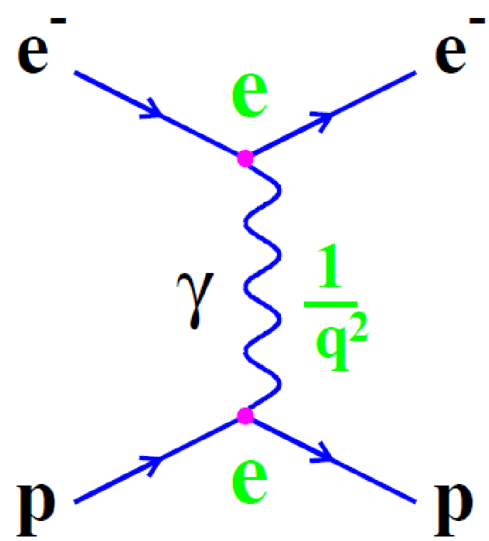

$$M = \frac{e^2}{q^2} = \frac{4\pi\alpha}{q^2}$$

$$\frac{d\sigma}{d\Omega} = \frac{\alpha^2}{4E^2 \sin^4\frac{\theta}{2}}$$

Електрон-позитронно разсейване

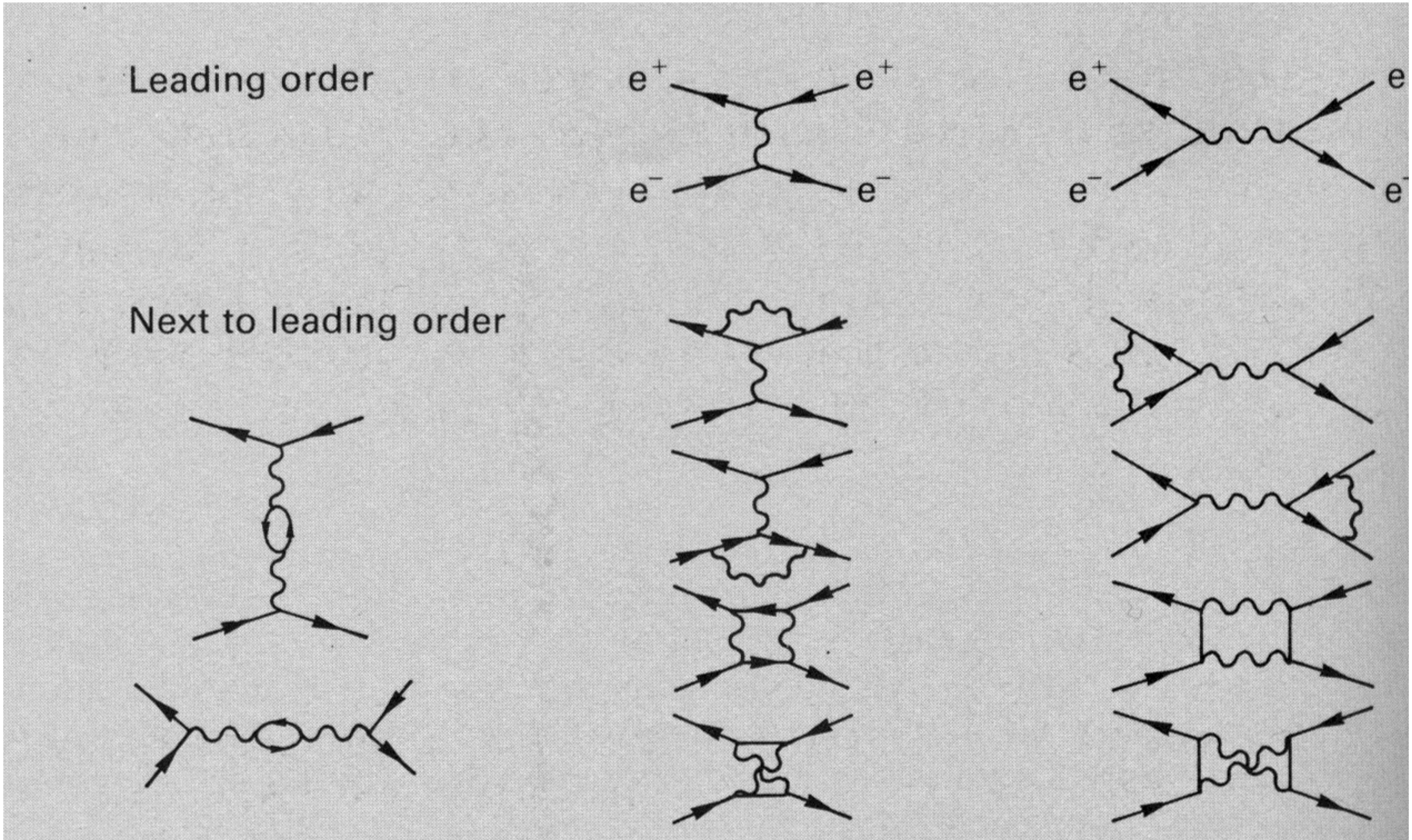

THE MUON ANOMALOUS MAGNETIC MOMENT

http://pdg.lbl.gov/2011/reviews/rpp2011-rev-g-2-muon-anom-mag-moment.pdf

$$\vec{M} = g_\mu \frac{e}{2m_\mu}\vec{S} \qquad g_\mu = 2 \qquad a_\mu \equiv \frac{g_\mu - 2}{2}$$

$$a_{\mu^+}^{\text{exp}} = 11\,659\,204(6)(5) \times 10^{-10}$$
$$a_{\mu^-}^{\text{exp}} = 11\,659\,215(8)(3) \times 10^{-10}$$

$$a_\mu^{\text{exp}} = 11\,659\,208.9(5.4)(3.3) \times 10^{-10}$$

$$a_\mu^{\mathrm{SM}} = a_\mu^{\mathrm{QED}} + a_\mu^{\mathrm{EW}} + a_\mu^{\mathrm{Had}}$$

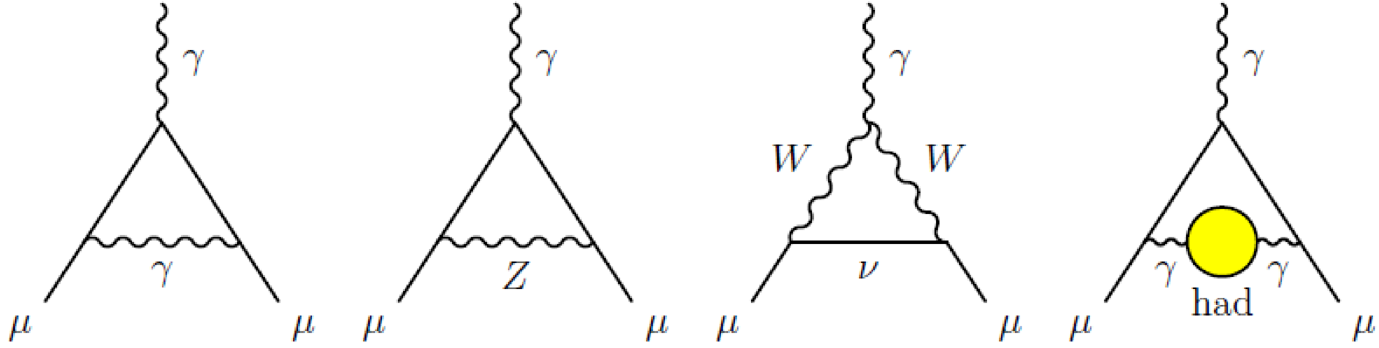

Figure 1: Representative diagrams contributing to a_μ^{SM}. From left to right: first order QED (Schwinger term), lowest-order weak, lowest-order hadronic.

$$a_\mu^{\rm QED} = \frac{\alpha}{2\pi} + 0.765857410(27)\left(\frac{\alpha}{\pi}\right)^2 + 24.05050964(43)\left(\frac{\alpha}{\pi}\right)^3 + 130.8055(80)\left(\frac{\alpha}{\pi}\right)^4 + 663(20)\left(\frac{\alpha}{\pi}\right)^5 + \cdots \quad (5)$$

$$\alpha^{-1} = 137.035999084(51)$$

$$a_\mu^{\rm QED} = 116\,584\,718.09(0.15) \times 10^{-11}$$

$$a_\mu^{\rm EW}[\text{1-loop}] = \frac{G_\mu m_\mu^2}{8\sqrt{2}\pi^2}\left[\frac{5}{3} + \frac{1}{3}\left(1 - 4\sin^2\theta_{\rm W}\right)^2 + \mathcal{O}\left(\frac{m_\mu^2}{M_W^2}\right) + \mathcal{O}\left(\frac{m_\mu^2}{m_H^2}\right)\right], = 194.8 \times 10^{-11},$$

$$a_\mu^{\rm EW}[\text{2-loop}] = -40.7(1.0)(1.8) \times 10^{-11}$$

$$a_\mu^{\rm EW} = 154(1)(2) \times 10^{-11}$$

Hadronic (quark and gluon) loop contributions to $a_\mu^{\rm SM}$ give rise to its main theoretical uncertainties. At present, those effects are not calculable from first principles, but such an approach, at least partially, may become possible as lattice QCD matures. Instead, one currently relies on a dispersion relation approach to evaluate the lowest-order (*i.e.*, $\mathcal{O}(\alpha^2)$) hadronic vacuum polarization contribution $a_\mu^{\rm Had}[{\rm LO}]$ from corresponding cross section measurements [13]

$$a_\mu^{\rm Had}[{\rm LO}] = \frac{1}{3}\left(\frac{\alpha}{\pi}\right)^2 \int\limits_{m_\pi^2}^{\infty} ds \, \frac{K(s)}{s} R^{(0)}(s) \,, \qquad (10)$$

where $K(s)$ is a QED kernel function [14], and where $R^{(0)}(s)$ denotes the ratio of the bare[2] cross section for e^+e^- annihilation into hadrons to the pointlike muon-pair cross section at center-of-mass energy $\sqrt{s}$. The function $K(s) \sim 1/s$ in Eq. (10) gives a strong weight to the low-energy part of the integral. Hence, $a_\mu^{\rm Had}[{\rm LO}]$ is dominated by the $\rho(770)$ resonance.

$$a_\mu^{\mathrm{Had}}[\mathrm{LO}] = 6\,955(40)(7) \times 10^{-11}\,, \tag{11}$$

where the first error is experimental (dominated by systematic uncertainties), and the second due to perturbative QCD,

Alternatively, one can use precise vector spectral functions from $\tau \to \nu_\tau +$ hadrons decays [16] that can be related to isovector $e^+e^- \to$ hadrons cross sections by isospin symmetry. When isospin-violating corrections (from QED and $m_d - m_u \neq 0$) are applied, one finds [17]

$$a_\mu^{\mathrm{Had}}[\mathrm{LO}] = 7\,053(40)(19)(7) \times 10^{-11}\ (\tau)\,, \tag{12}$$

where the first error is experimental, the second estimates the uncertainty in the isospin-breaking corrections applied to the τ data, and the third error is due to perturbative QCD. The discrepancy between the e^+e^- and τ-based determinations of

Higher order, $\mathcal{O}(\alpha^3)$, hadronic contributions are obtained from dispersion relations using the same $e^+e^- \to$ hadrons data [16,18,21], giving $a_\mu^{\mathrm{Had,Disp}}[\mathrm{NLO}] = (-98 \pm 1) \times 10^{-11}$, along with model-dependent estimates of the hadronic light-by-light scattering contribution, $a_\mu^{\mathrm{Had,LBL}}[\mathrm{NLO}]$, motivated by large-$N_C$ QCD [22–28]. [3] Following [26], one finds for the sum of the two terms

$$a_\mu^{\mathrm{Had}}[\mathrm{NLO}] = 7(26) \times 10^{-11}\,, \tag{13}$$

where the error is dominated by hadronic light-by-light uncertainties.

$$a_\mu^{\mathrm{SM}} = 116\,591\,834(2)(41)(26) \times 10^{-11}$$

$$\Delta a_\mu = a_\mu^{\text{exp}} - a_\mu^{\text{SM}} = 255(63)(49) \times 10^{-11}\,, \qquad (15)$$

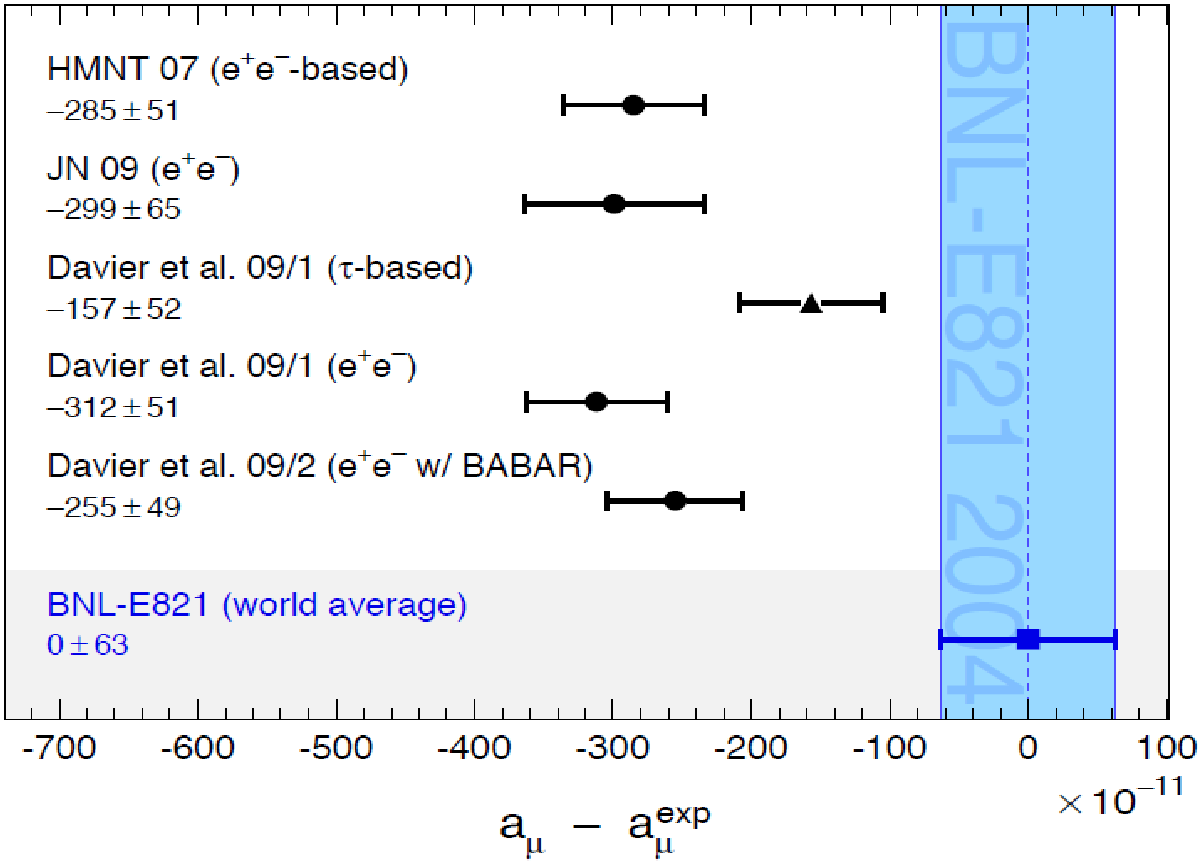

Figure 2: Compilation of recently published results for a_μ (in units of 10^{-11}), subtracted by the central value of the experimental aver-

An alternate interpretation is that Δa_μ may be a new physics signal with supersymmetric particle loops as the leading candidate explanation. Such a scenario is quite natural, since generically, supersymmetric models predict [1] an additional contribution to $a_\mu^{\rm SM}$

$$a_\mu^{\rm SUSY} \simeq \pm 130 \times 10^{-11} \cdot \left(\frac{100\ \text{GeV}}{m_{\rm SUSY}}\right)^2 \tan\beta\,, \qquad (16)$$

where $m_{\rm SUSY}$ is a representative supersymmetric mass scale, and $\tan\beta \simeq 3$–40 is a potential enhancement factor. Supersymmetric particles in the mass range 100–500 GeV could be the source of the deviation Δa_μ. If so, those particles could be directly observed at the next generation of high energy colliders. New physics effects [1] other than supersymmetry could also explain a non-vanishing Δa_μ.

Разсейване на електрон от зарядово разпределение

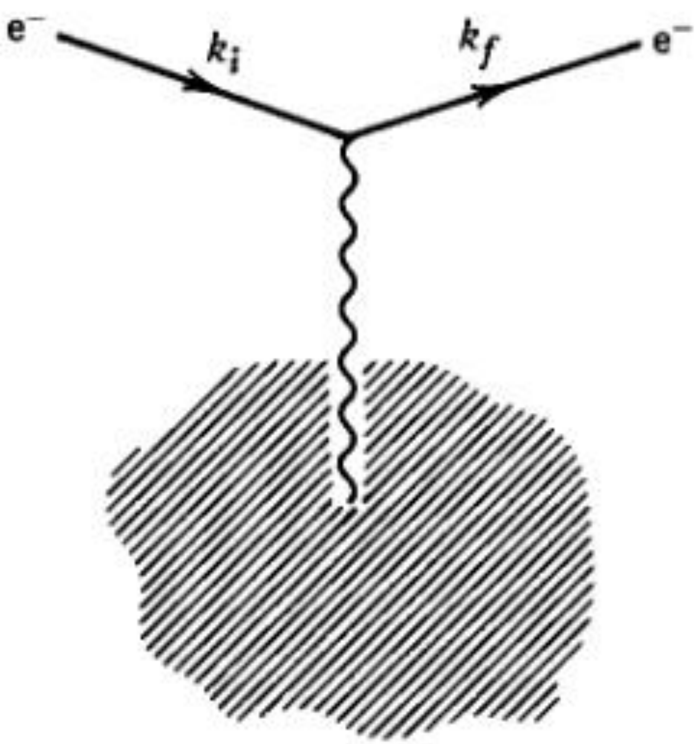

$$\frac{d\sigma}{d\Omega} = \left(\frac{d\sigma}{d\Omega}\right)_{\text{point}} \left|F(q)\right|^2,$$

Експерименти по разсейване

Оптически аналог – снемане на дифракционна картина, която отразява масовото или зарядовото разпределение на ядрената материя

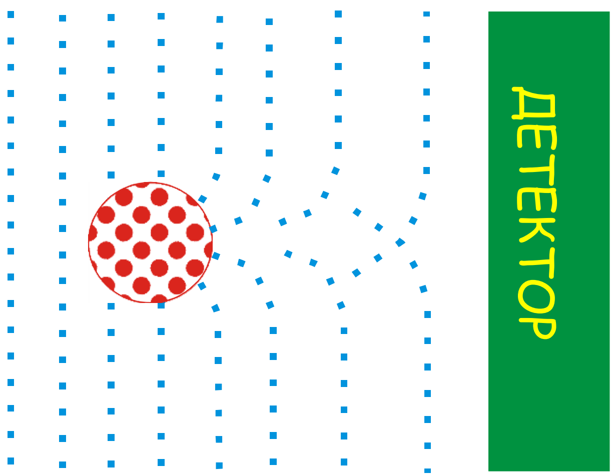

Фрауенхоферова дифракция

D – диаметър на ядрото

$$D \sin\Theta = m\lambda$$

	$m_{minimum}$	$m_{maximum}$
1	1.22	1.63
2	2.23	2.68
3	3.28	3.69

$$\lambda = \frac{h}{p} \leqslant D \qquad \lambda = \frac{2\pi\,(197.3)}{E_e\,[\mathrm{MeV}]}\,[\mathrm{fm}]$$

Обект	Скала [fm]	Енергия на електрона [MeV]
Атом	10^5	0.01
Тежко ядро (Pb)	10	100
Протон	1	1000
Кварки	0.1 ?	10000

Резултати от (e,e') експерименти

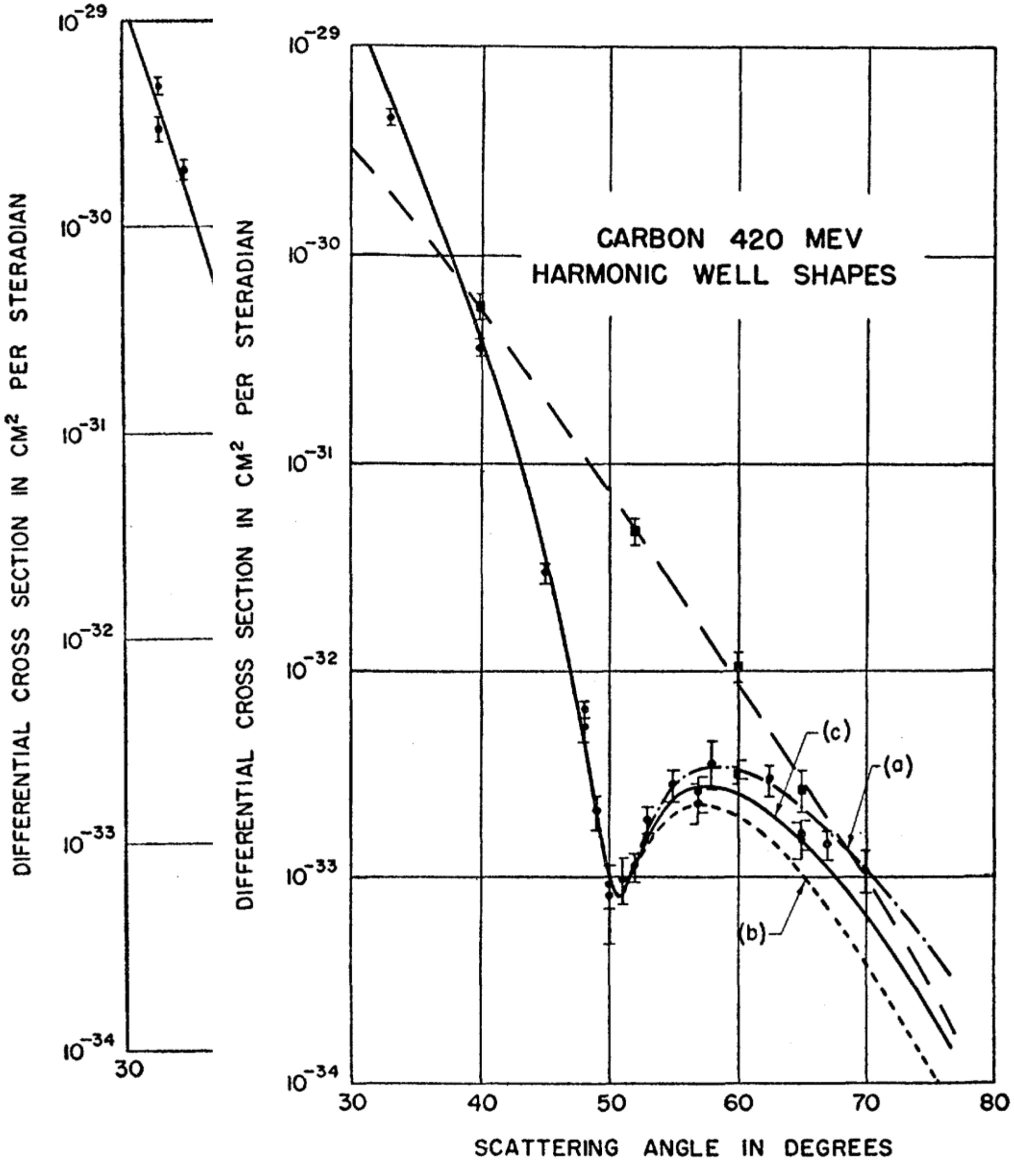

Ehrenberg *et al.*, Phys. Rev. **113**, 666 (1959)

E_e = 420 MeV ⇒ λ = 2.9 fm

$\theta = 42^\circ$

D.Sin (θ) = 1.22 λ

D = 5.28 fm

r (^{16}O) = 2.64 fm

$\theta = 51^\circ$

D = 4.56 fm

r (^{12}C) = 2.28 fm

Еластично разсейване - квантово механично описание

$e^{i\vec{k}_i.\vec{r}}$

$\vec{p}_i = \hbar\,\vec{k}_i$

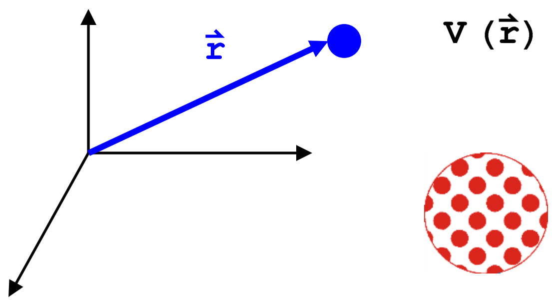

$e^{i\vec{k}_f.\vec{r}}$

$\vec{p}_f = \hbar\,\vec{k}_f$

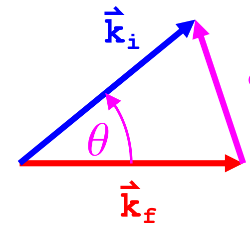

$\vec{q} = \hbar\left(\vec{k}_i - \vec{k}_f\right) = \vec{p}_i - \vec{p}_f$

$|\vec{p}_i| = |\vec{p}_f|$

Златно правило на Ферми: $\lambda\left(\vec{k}_i, \vec{k}_f\right) = \dfrac{2\pi}{\hbar}\left|M\left(\vec{k}_i, \vec{k}_f\right)\right|^2 \rho\,(E_f) \quad (s^{-1})$

$$\equiv \langle \psi_f \,|\, V(\vec{r}) \,|\, \psi_i \rangle \equiv \langle f \,|\, V(\vec{r}) \,|\, i \rangle$$

$$M\left(\vec{k}_i, \vec{k}_f\right) = \frac{1}{V}\int \psi_f^* \, V(\vec{r})\, \psi_i \, d\vec{r} = \frac{1}{V}\int e^{-i\vec{k}_f.\vec{r}}\, V(\vec{r})\, e^{i\vec{k}_i.\vec{r}}\, d\vec{r} = \frac{1}{V}\int e^{i\left(\vec{k}_i - \vec{k}_f\right).\vec{r}}\, V(\vec{r})\, d\vec{r}$$

$$d\sigma(\theta, \varphi) = \frac{m^2}{\pi\,\hbar^4} M_{fi}^2 \frac{d\Omega}{4\pi}$$

$$\frac{d\sigma}{d\Omega}(\theta, \varphi) = \frac{m^2}{4\pi^2\hbar^4} M_{fi}^2 = |f(\theta)|^2$$

$f(\theta)$ – амплитуда на разсейване

$$\boxed{f(\theta) = \frac{m}{2\pi\hbar^2}\int V(\vec{r})\, e^{\frac{i}{\hbar}\vec{q}.\vec{r}}\, d\vec{r}}$$

Еластично разсейване от централен потенциал

$$e^{i\vec{k}_i.\vec{r}} \qquad \vec{p}_i = \hbar\vec{k}_i$$

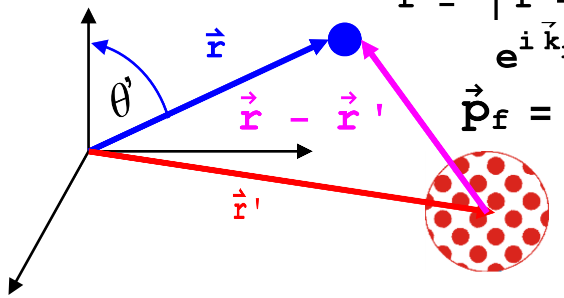

$$V(\vec{r}) = V(r) \qquad r = |\vec{r} - \vec{r}\,'|$$

$$e^{i\vec{k}_f.\vec{r}} \qquad \vec{p}_f = \hbar\vec{k}_f$$

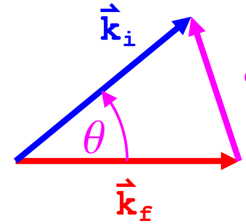

$$\vec{q} = \hbar(\vec{k}_i - \vec{k}_f) = \vec{p}_i - \vec{p}_f \qquad |\vec{p}_i| = |\vec{p}_f|$$

$$\boxed{f(\theta) = \frac{m}{2\pi\hbar^2}\int V(\vec{r})\, e^{\frac{i}{\hbar}\vec{q}.\vec{r}}\, d\vec{r}}$$

$$\vec{q}.\vec{r} = q\,r\cos\theta' \qquad d\vec{r} = r^2\sin\theta'\,dr\,d\theta'\,d\varphi$$

$$f(\theta) = \frac{m}{2\pi\hbar^2}\int_r V(r)\,r^2\,dr\int_{\varphi'} d\varphi'\int_{\theta'} e^{\frac{i}{\hbar}q\,r\cos\theta'}\sin\theta'\,d\theta'$$

$$\int_0^\pi e^{\frac{i}{\hbar}q.r\cos\theta'}\sin\theta'\,d\theta' = -\frac{\hbar}{iqr}\int_0^\pi e^{\frac{i}{\hbar}q\,r\cos\theta'}\,d\left(\frac{i}{\hbar}q\,r\cos\theta'\right) = \frac{\hbar}{iqr}\int_{-\frac{i}{\hbar}qr}^{\frac{i}{\hbar}qr} e^{\xi}\,d\xi =$$

$$= \frac{\hbar}{iqr}(2i)\frac{e^{\frac{i}{\hbar}qr} - e^{-\frac{i}{\hbar}qr}}{(2i)} = \frac{2\sin(qr/\hbar)}{(qr/\hbar)}$$

$$f(\theta) = \frac{m}{2\pi\hbar^2}\,2\pi\,\frac{2\hbar}{q}\int_0^\infty \frac{\sin(qr/\hbar)}{r}V(r)\,r^2\,dr \;\boxed{= \frac{2m}{q\hbar}\int_0^\infty \sin(qr/\hbar)\,V(r)\,r\,dr}$$

Ръдърфордовско разсейване от точков обект

$$V(r) = \frac{Ze^2}{4\pi\epsilon_0}\frac{1}{r}$$

$$f(\theta) = \frac{2m}{q\hbar}\frac{Ze^2}{4\pi\epsilon_0}\int_0^\infty \sin(qr/\hbar)\,dr = \frac{2m}{q\hbar}\frac{Ze^2}{4\pi\epsilon_0}\lim_{a\to 0}\int_0^\infty \sin(qr/\hbar)\,e^{-ra}\,dr = \frac{2m}{q\hbar}\frac{Ze^2}{4\pi\epsilon_0}\frac{\hbar}{q} = \frac{2m}{q^2}\frac{Ze^2}{4\pi\epsilon_0}$$

$$\lim_{a\to 0}\int_0^\infty \sin(bx)\,e^{-ax}\,dx = \lim_{a\to 0}\frac{b}{a^2+b^2} = \frac{1}{b}$$

$$\frac{d\sigma}{d\Omega} = |f(\theta)|^2 \;\boxed{= \frac{4m^2}{q^4}\left(\frac{Ze^2}{4\pi\epsilon_0}\right)^2}$$

$$q = 2p\sin(\theta/2)$$

$$p = |\vec{p}_i| = |\vec{p}_f|$$

$$E = p^2/2m$$

изика/20

$$\frac{d\sigma}{d\Omega} = \left(\frac{Zz'e^2}{4\pi\epsilon_0}\right)^2\left(\frac{1}{4E}\right)^2\frac{1}{\sin^4(\theta/2)}$$

Еластично разсейване от обект с крайни размери

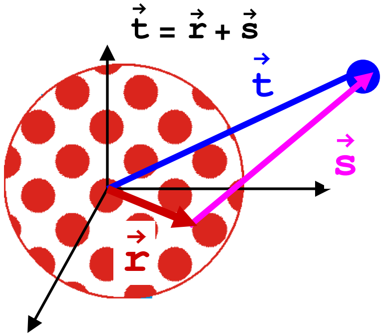

$$dV = \left(\frac{Ze^2}{4\pi\epsilon_0}\right)\frac{\rho(r)}{s}\,d\vec{r}$$

$$\boxed{f(\theta) = \frac{m}{2\pi\hbar^2}\int V(\vec{r})\, e^{\frac{i}{\hbar}\vec{q}\cdot\vec{r}}\, d\vec{r}}$$

$$f(\theta) = \frac{m}{2\pi\hbar^2}\left(\frac{Ze^2}{4\pi\epsilon_0}\right)\iint \frac{\rho(r)}{s}\, e^{\frac{i}{\hbar}\vec{q}\cdot\vec{t}}\, d\vec{t}\, d\vec{s}$$

$$= \frac{m}{2\pi\hbar^2}\left(\frac{Ze^2}{4\pi\epsilon_0}\right)\iint \frac{\rho(r)}{s}\, e^{\frac{i}{\hbar}\vec{q}\cdot(\vec{r}+\vec{s})}\, d\vec{r}\, d\vec{s} = \int \rho(r)\, e^{\frac{i}{\hbar}\vec{q}\cdot\vec{r}}\, d\vec{r}\; \frac{m}{2\pi\hbar^2}\left(\frac{Ze^2}{4\pi\epsilon_0}\right)\int \frac{e^{\frac{i}{\hbar}\vec{q}\cdot\vec{s}}}{s}\, d\vec{s}$$

$$= \underbrace{\int_0^\infty \rho(r)\,\frac{\sin(qr/\hbar)}{(qr/\hbar)}\,4\pi r^2\, dr}_{F(q)} \times \underbrace{\frac{2m}{q\hbar}\left(\frac{Ze^2}{4\pi\epsilon_0}\right)\int_0^\infty \sin(qs/\hbar)\, ds}_{f(\theta)_{Ruth}}$$

$$\frac{d\sigma}{d\Omega} = |f(\theta)|^2 = F^2(q)\left(\frac{d\sigma}{d\Omega}\right)_{Ruth}$$

Фурие образ на ядрената зарядова плътност

$F(q)$ – ядрен форм-фактор

при разсейване от твърда сфера
се получават минимуми и максимуми.

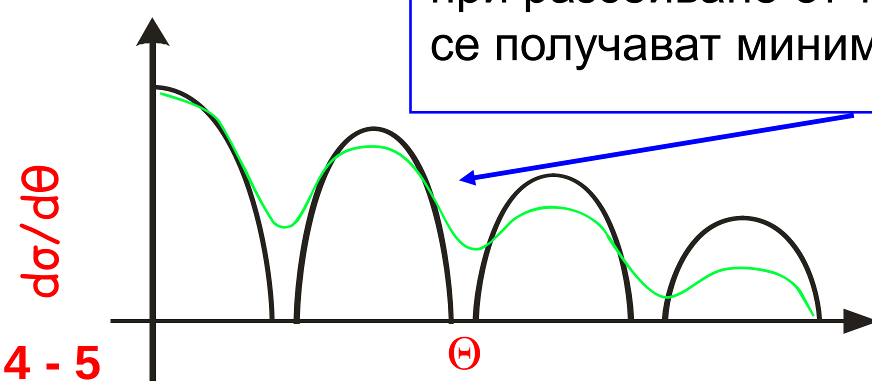

Резултати от (e,e’) експерименти

Релативистки частици
откат на ядрото
Допълнителни взаимодействия

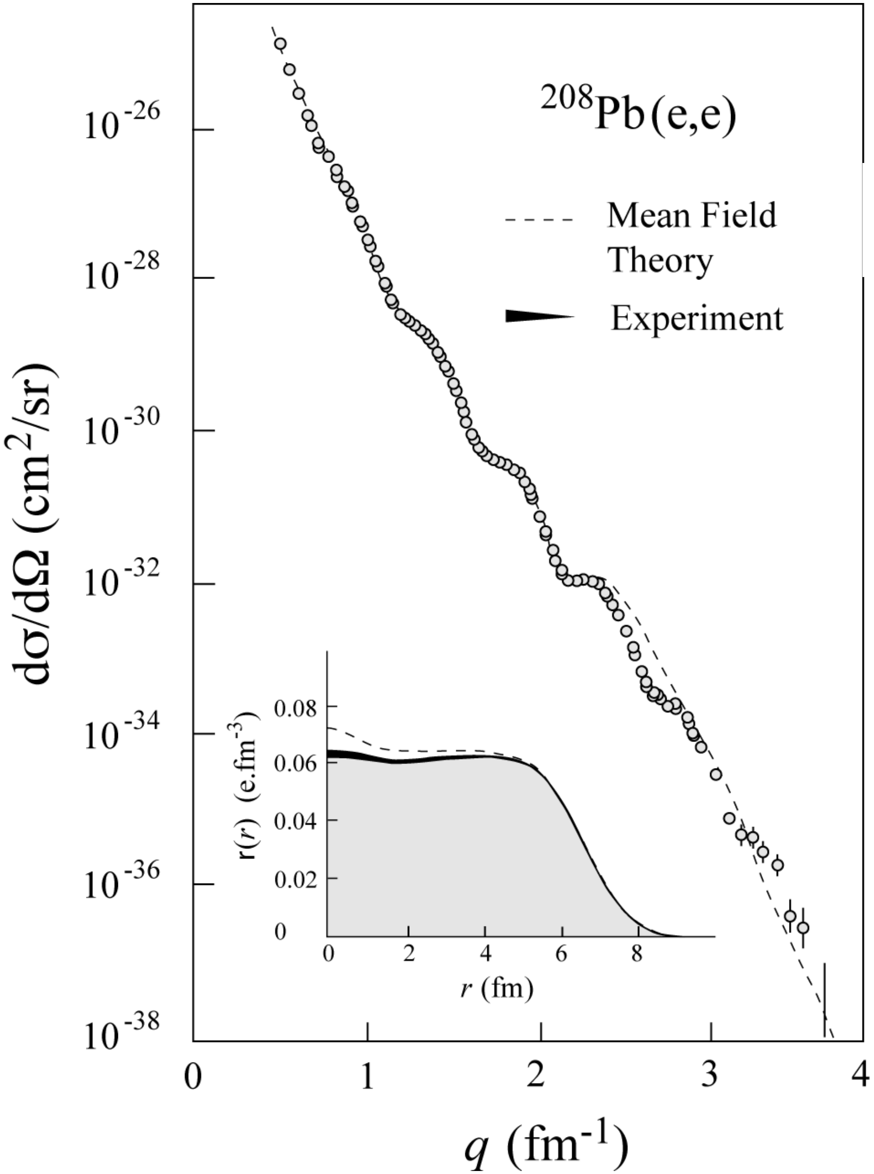

$$\left(\frac{d\sigma}{d\Omega}\right)_{Mott} = \left(\frac{d\sigma}{d\Omega}\right)_{Rutherford} \left(1 - \beta^2 \sin^2 \frac{\theta}{2}\right)$$

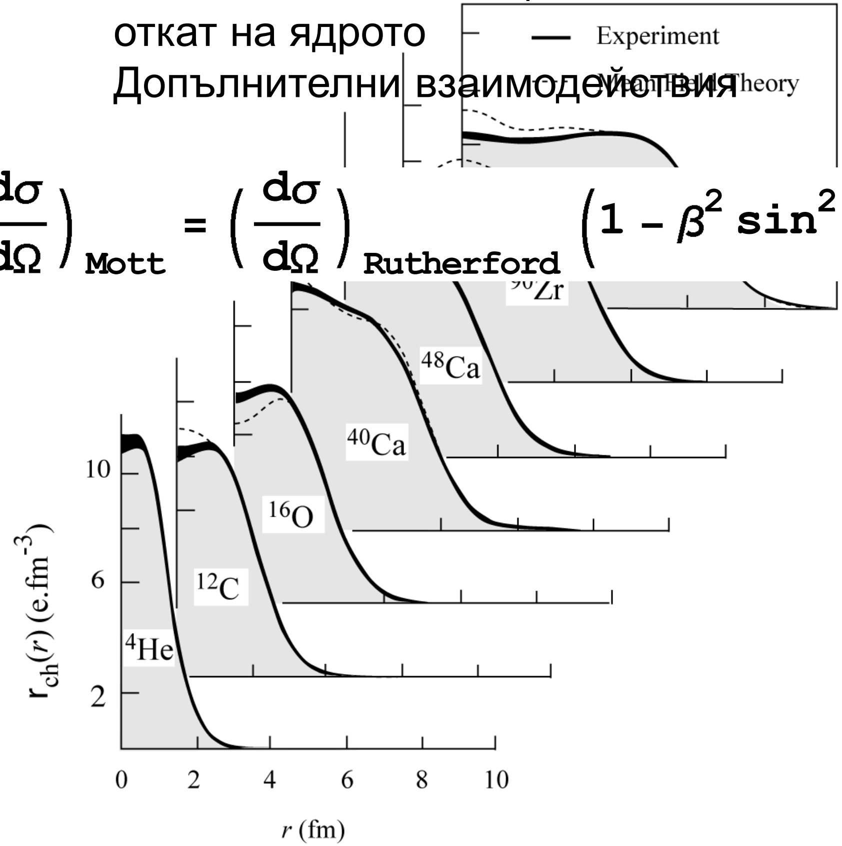

$R=1.23(1)A^{1/3}$[fm]

$d \approx 2.3$ fm

Ядрен радиус

Функция на Ферми

$$\rho(r) = \rho(0)\left[1 + \mathrm{Exp}\left(\frac{r-R}{a}\right)\right]^{-1}$$

$$\frac{A}{\frac{4}{3}\pi R^3} \sim \text{constant}$$

$$R = \text{const} \,.\, A^{1/3}$$

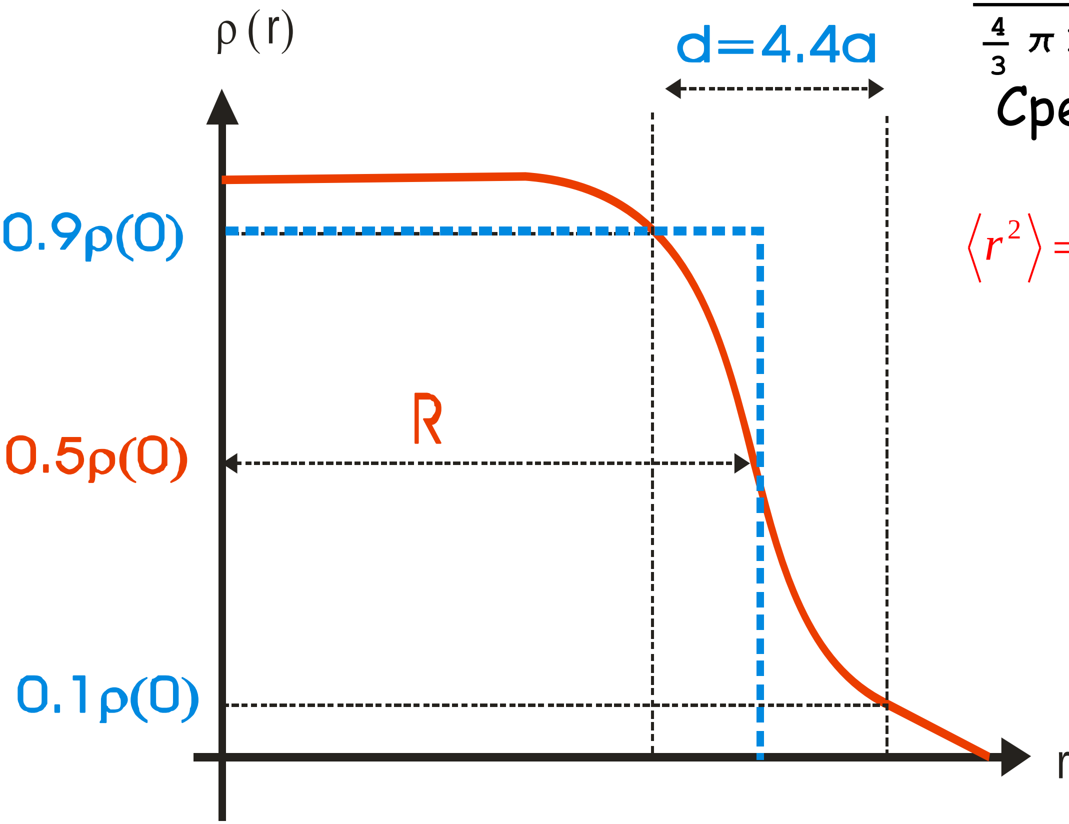

Средно-квадратичен радиус

$$\langle r^2\rangle = \frac{\int \rho(r) r^2 d^3 r}{\int \rho(r) d^3 r}$$

$$\langle r^2\rangle^{1/2} \neq R$$

$$\rho(r) = \begin{cases} \rho_0 & r \leqslant R \\ 0 & r > R \end{cases}$$

$$\int \rho(r)\, d^3 r = \int_0^\infty \rho(r)\, r^2\, dr \int_\Omega d\Omega$$

$$= \rho_0\, 4\pi \int_0^R r^2\, dr = \frac{4\pi}{3} \rho_0 R^3$$

$$\int \rho(r)\, r^2\, d^3 r = \int_0^\infty \rho(r)\, r^4\, dr \int_\Omega d\Omega = \rho_0\, 4\pi \int_0^R r^4\, dr = \frac{4\pi}{5}\rho_0 R^5$$

$$\langle r^2\rangle = \frac{3}{5} R^2$$

$$R_{rms} = \left(\frac{5}{3}\langle r^2\rangle\right)^{1/2}$$

Средно-квадратичен радиус при функция на Ферми

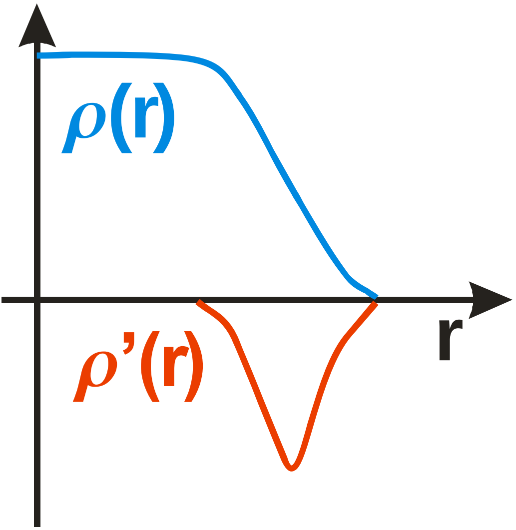

$$\rho(r) = \rho(0)\left[1 + \mathrm{Exp}\left(\frac{r-R}{a}\right)\right]^{-1}$$

$$\langle r^2 \rangle = 4\pi\rho_0 R^2 \frac{3}{5}\left[1 + \frac{7\pi^2}{6}\left(\frac{a}{R}\right)^2\right]$$

$R_{rms} \to R$ когато $a/R \to 0$

$a \approx 0.55 \div 0.60$ fm $\to$ 10% ефект

$$\boxed{R_{rms} \approx 1.2 x A^{1/3}\ \mathrm{fm}}$$

$$\left(\frac{d\sigma}{d\Omega}\right)_{\text{point}} \equiv \left(\frac{d\sigma}{d\Omega}\right)_{\text{Mott}} = \frac{(Z\alpha)^2 E^2}{4k^4 \sin^4 \frac{\theta}{2}}\left(1 - v^2 \sin^2 \frac{\theta}{2}\right)$$

$$F(\mathbf{q}) = \int \left(1 + i\mathbf{q}\cdot\mathbf{x} - \frac{(\mathbf{q}\cdot\mathbf{x})^2}{2} + \cdots\right)\rho(\mathbf{x})\, d^3x$$
$$= 1 - \frac{1}{6}|\mathbf{q}|^2\langle r^2\rangle + \cdots,$$

- При разсейване от протон има усложнения

$$\left.\frac{d\sigma}{d\Omega}\right|_{\text{lab}} = \left(\frac{\alpha^2}{4E^2\sin^4\frac{\theta}{2}}\right)\frac{E'}{E}\left\{\left(F_1^2 - \frac{\kappa^2 q^2}{4M^2}F_2^2\right)\cos^2\frac{\theta}{2} - \frac{q^2}{2M^2}(F_1 + \kappa F_2)^2\sin^2\frac{\theta}{2}\right\}$$

$$G_E \equiv F_1 + \frac{\kappa q^2}{4M^2}F_2$$

$$G_M \equiv F_1 + \kappa F_2,$$

$$\left.\frac{d\sigma}{d\Omega}\right|_{\mathrm{lab}} = \frac{\alpha^2}{4E^2 \sin^4 \frac{\theta}{2}} \frac{E'}{E} \left(\frac{G_E^2 + \tau G_M^2}{1+\tau} \cos^2 \frac{\theta}{2} + 2\tau G_M^2 \sin^2 \frac{\theta}{2} \right)$$

$$\tau \equiv -q^2/4M^2$$

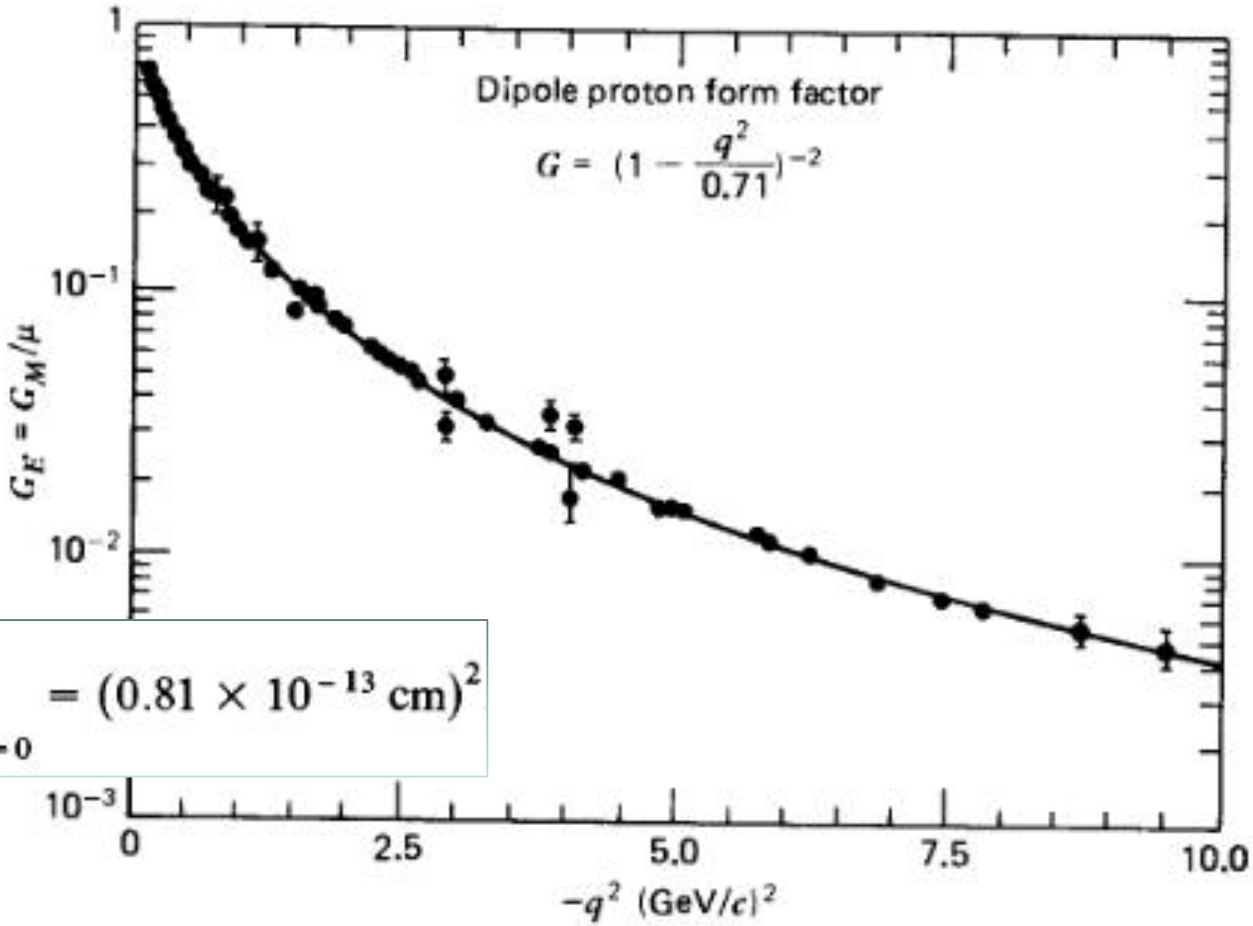

$$\langle r^2 \rangle = 6 \left(\frac{dG_E(q^2)}{dq^2} \right)_{q^2=0} = (0.81 \times 10^{-13}\ \mathrm{cm})^2$$

Fig. 8.4 The proton form factors as a function of q^2.

Нееластично разсейване на електрон от обект с разпределен заряд

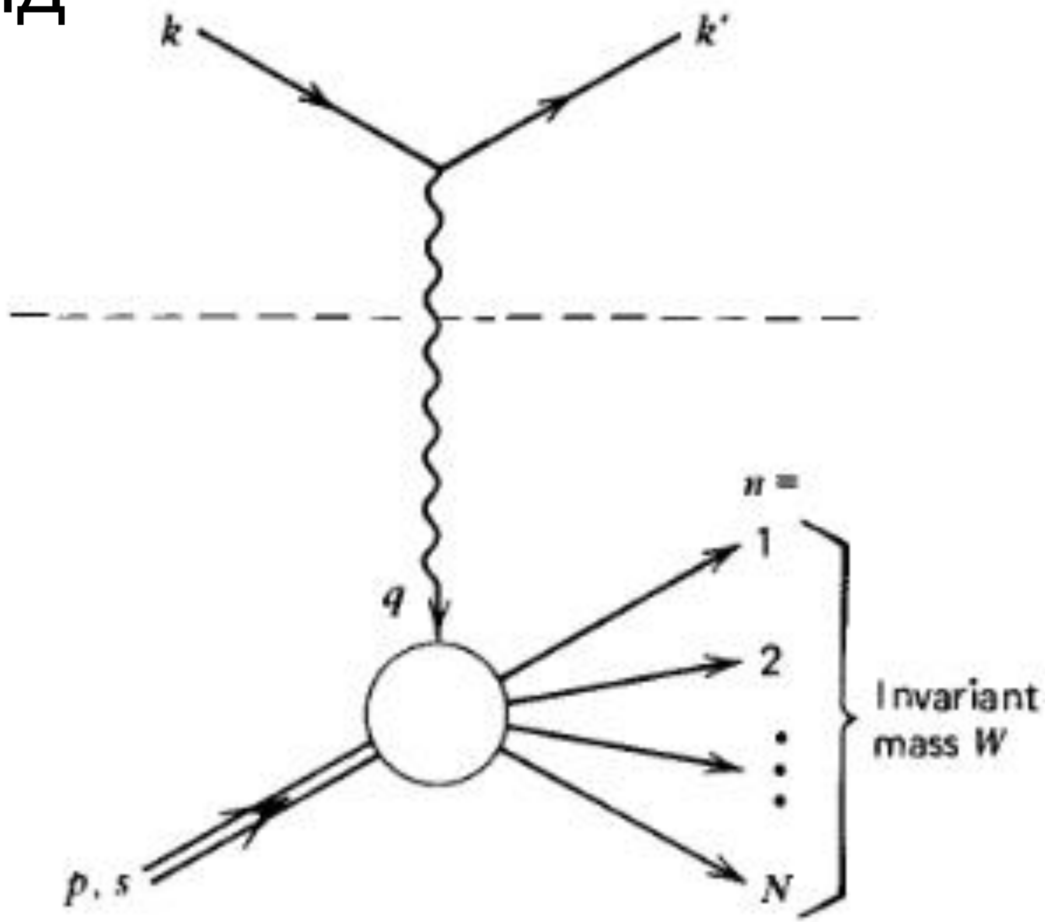

31

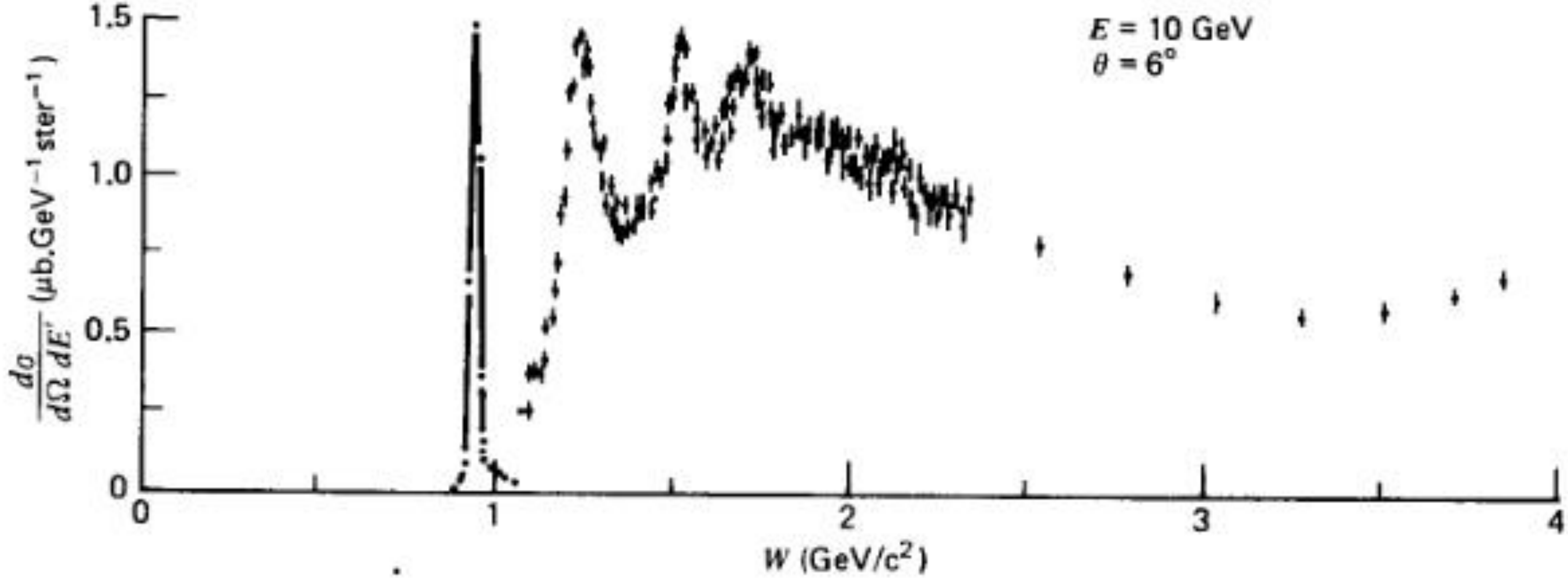

Fig. 8.6 The ep → eX cross section as a function of the missing mass W. Data are from the Stanford Linear Accelerator. The elastic peak at $W = M$ has been reduced by a factor of 8.5.

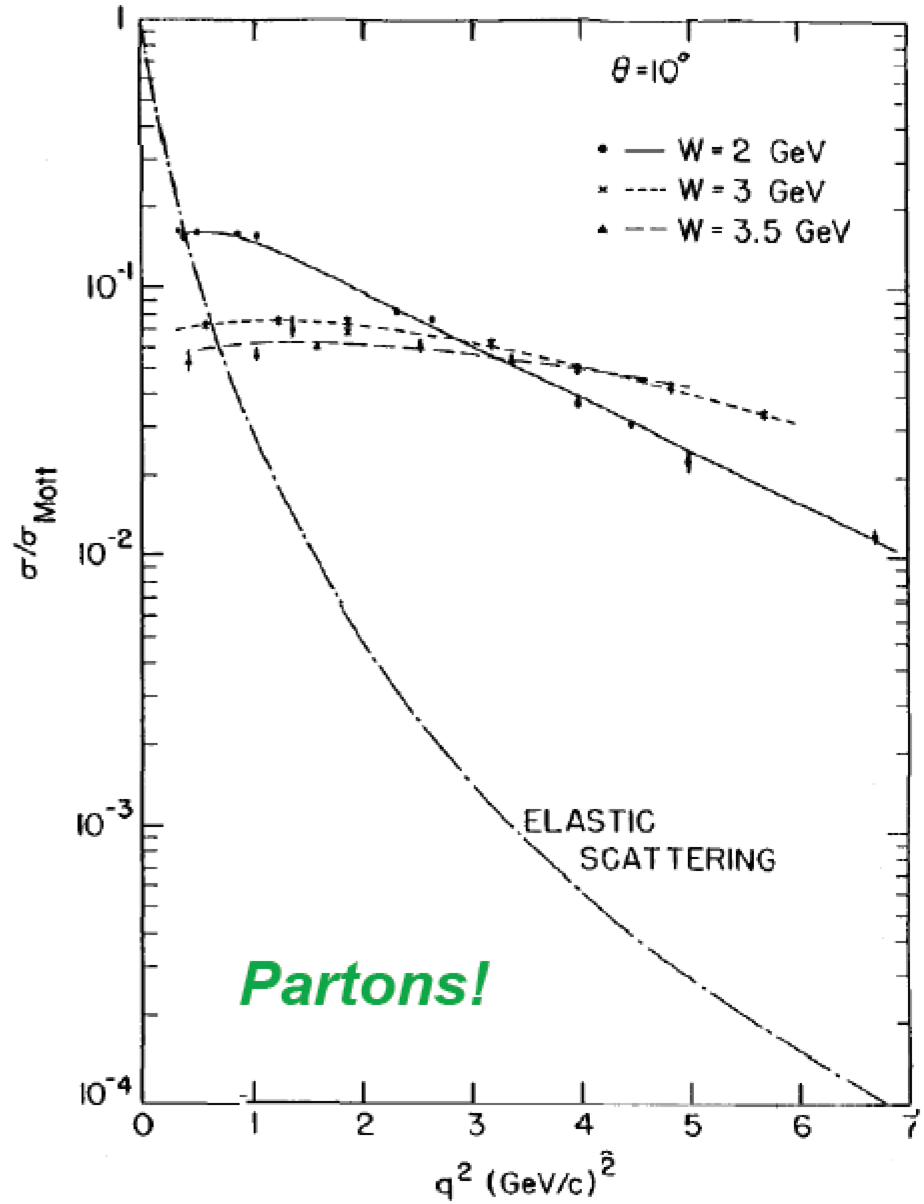

θ=10°
W = 2 GeV
W = 3 GeV
W = 3.5 GeV
ELASTIC SCATTERING
Partons!
σ/σ_Mott
q² (GeV/c)²

Нееластично *ep* разсейване – кинематични променливи:

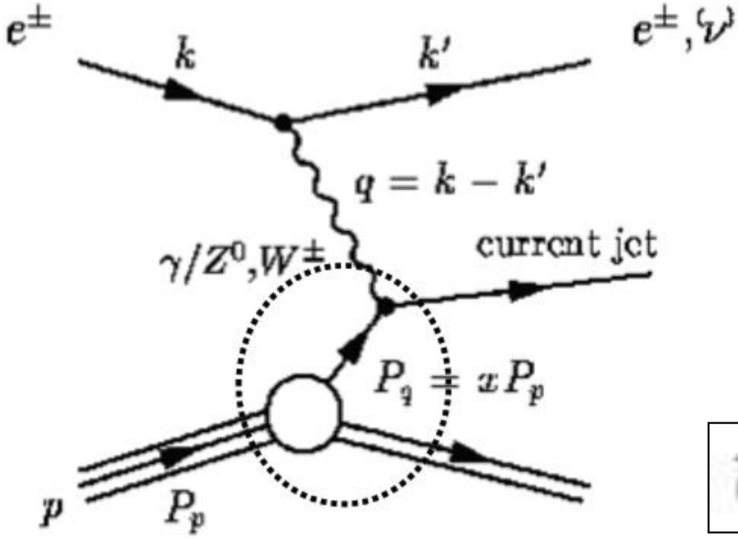

$$\boxed{q^2}$$

$$\boxed{\nu \equiv \frac{p \cdot q}{M}}$$

$$\boxed{W^2 = (p+q)^2 = M^2 + 2M\nu + q^2}$$

$$\boxed{x = \frac{-q^2}{2p \cdot q} = \frac{-q^2}{2M\nu}, \qquad y = \frac{p \cdot q}{p \cdot k}}$$

$$\boxed{\left.\frac{d\sigma}{dE'\,d\Omega}\right|_{\text{lab}} = \frac{\alpha^2}{4E^2 \sin^4 \frac{\theta}{2}} \left\{ W_2(\nu, q^2) \cos^2 \frac{\theta}{2} + 2W_1(\nu, q^2) \sin^2 \frac{\theta}{2} \right\},}$$

- Можем ли с фотони с достатъчно малка дължина на вълната да “видим” какво има в протона ?
- Оказва се, че при нарастване на предадения при взаимодействието импулс протонът започва да изглежда като съставен от (квази)свободни Диракови частици (кварки);
- Нееластичното e-p разсейване тогава може да се опише като некохерентна сума от еластични e-q разсейвания:

- При прехода от сечение за разсейване от пространствено протяжен обект към сечение за разсейване от точкова частица структурните функции се трансформират в:

$$2W_1^{\text{point}} = \frac{Q^2}{2m^2}\delta\left(\nu - \frac{Q^2}{2m}\right),$$

$$W_2^{\text{point}} = \delta\left(\nu - \frac{Q^2}{2m}\right).$$

$$2mW_1^{\text{point}}(\nu, Q^2) = \frac{Q^2}{2m\nu}\delta\left(1 - \frac{Q^2}{2m\nu}\right),$$

$$\nu W_2^{\text{point}}(\nu, Q^2) = \delta\left(1 - \frac{Q^2}{2m\nu}\right).$$

Получаваме структурни функции, зависещи единствено от безразмерната променлива

$$Q^2/2m\nu$$

$$MW_1(\nu, Q^2) \xrightarrow[\text{large } Q^2]{} F_1(\omega),$$

$$\nu W_2(\nu, Q^2) \xrightarrow[\text{large } Q^2]{} F_2(\omega),$$

$$\omega = \frac{2q \cdot p}{Q^2} = \frac{2M\nu}{Q^2}, \qquad x = \frac{1}{\omega} = \frac{Q^2}{2M\nu}$$

37

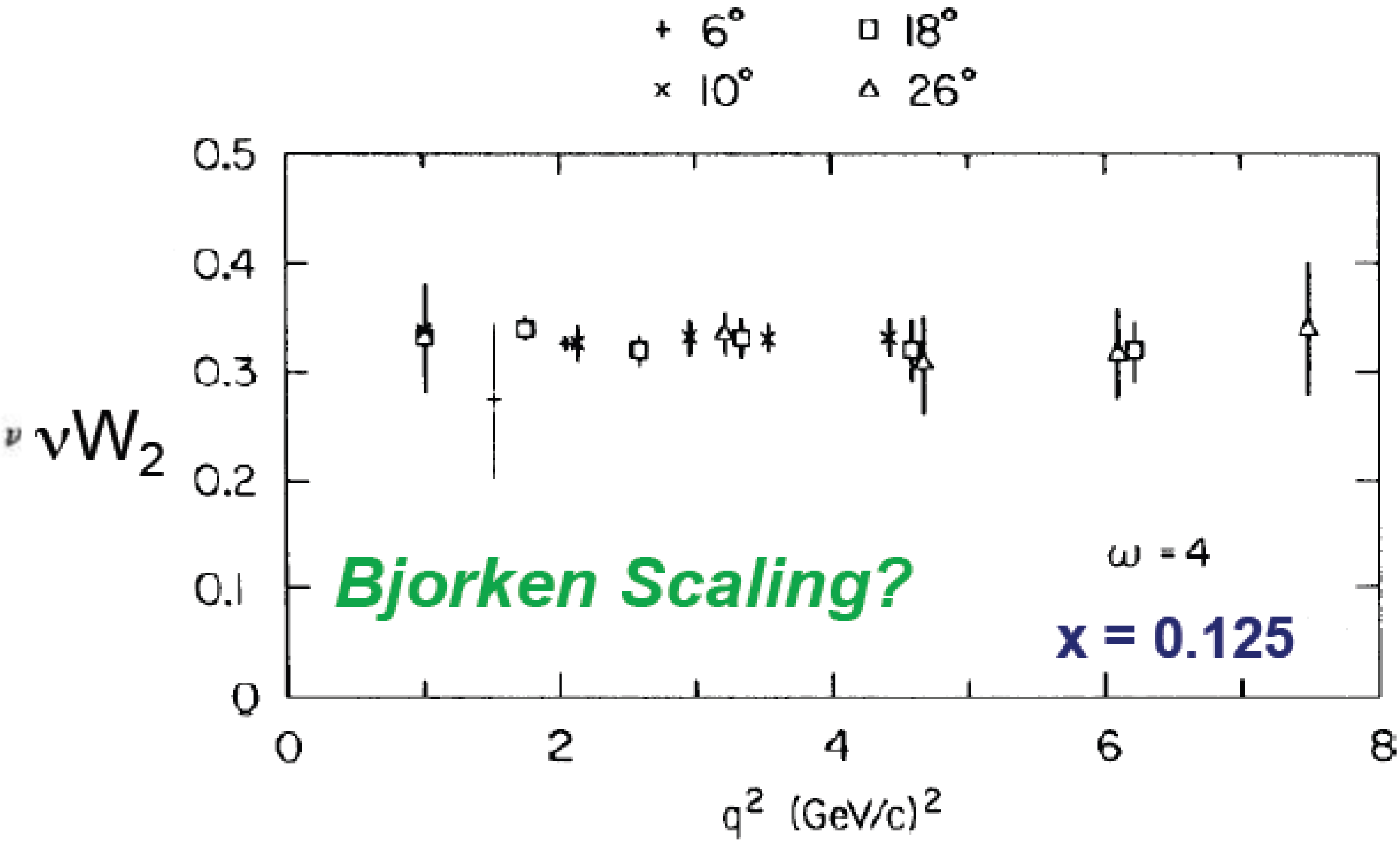

Fig. 9.2 The structure function νW_2 determined by electron–proton scattering as a function of Q^2 for $\omega = 4$. Data are from the Stanford Linear Accelerator.

- Основавайки се на експерименталните факти, разглеждаме протона като съставен от множество “партони”;
- Сечението за разсейване от протон може да се представи като следната некохерентна сума:

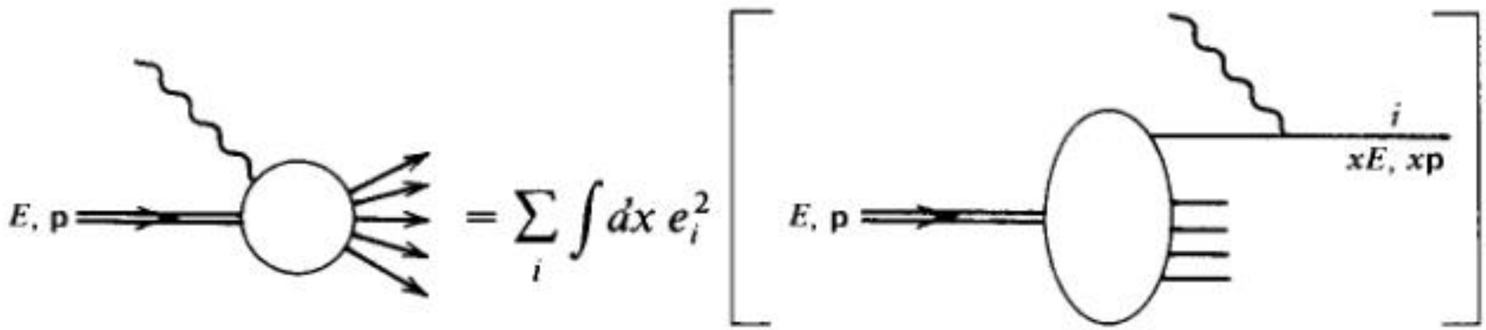

Функция на разпределение на партоните по импулси :

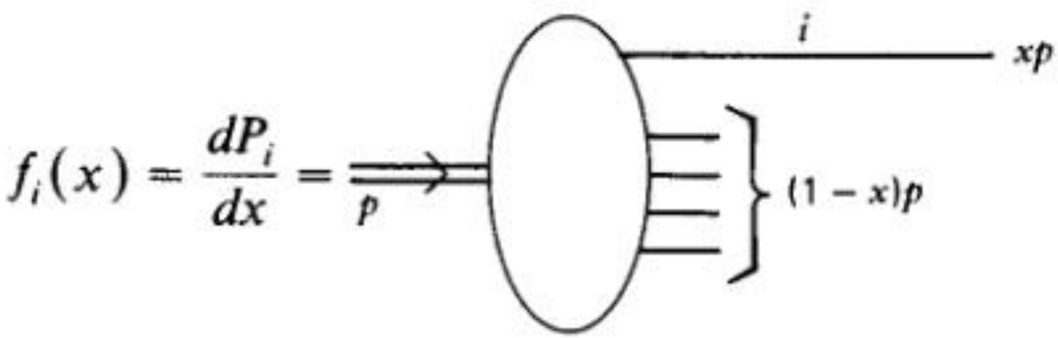

- Използвайки част от резултатите дотук стигаме до следния вид на структурните функции на протона:

$$\boxed{\begin{aligned} \nu W_2(\nu, Q^2) &\to F_2(x) = \sum_i e_i^2 x f_i(x), \\ M W_1(\nu, Q^2) &\to F_1(x) = \frac{1}{2x} F_2(x), \end{aligned}}$$

$$x = \frac{1}{\omega} = \frac{Q^2}{2M\nu}$$

- Оказва се, че кинематичната променлива $x_B \equiv x$ съвпада с частта от импулса на протона, носена от кварка;
- При фиксирано x_B структурните функции не зависят от предадения импулс – това е т.нар. Бьоркеновски скейлинг (scaling). *(Често това свойство се нарича* ***мащабна инвариантност****.)*

$$\frac{1}{x}F_2^{ep}(x) = \left(\frac{2}{3}\right)^2[u^p(x) + \bar{u}^p(x)] + \left(\frac{1}{3}\right)^2[d^p(x) + \bar{d}^p(x)]$$

$$+\left(\frac{1}{3}\right)^2[s^p(x) + \bar{s}^p(x)],$$

$$\frac{1}{x}F_2^{en} = \left(\frac{2}{3}\right)^2[u^n + \bar{u}^n] + \left(\frac{1}{3}\right)^2[d^n + \bar{d}^n] + \left(\frac{1}{3}\right)^2[s^n + \bar{s}^n];$$

Тук има 6 неизвестни кваркови разпределения.

Можем да използваме факта, че протонът и неутронът образуват изоспинов дублет:

$$u^p(x) = d^n(x) \equiv u(x),$$
$$d^p(x) = u^n(x) \equiv d(x),$$
$$s^p(x) = s^n(x) \equiv s(x).$$

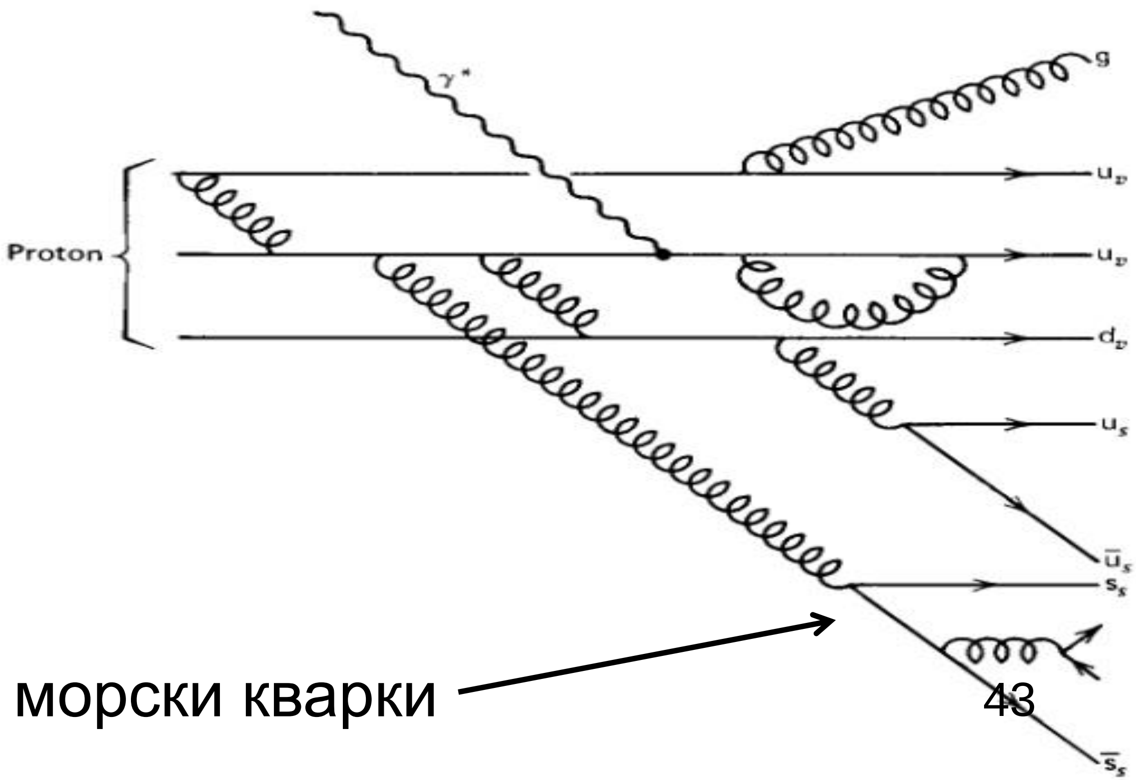

Валентни и морски кварки

Разпределения на валентните и морски кварки:

$$u_s(x) = \bar{u}_s(x) = d_s(x) = \bar{d}_s(x) = s_s(x) = \bar{s}_s(x) = S(x),$$
$$u(x) = u_v(x) + u_s(x),$$
$$d(x) = d_v(x) + d_s(x),$$

При сумиране на приносите от всички кварки трябва да се възстановяват квантовите числа на протона:

$$\int_0^1 [u(x) - \bar{u}(x)]\, dx = 2,$$
$$\int_0^1 [d(x) - \bar{d}(x)]\, dx = 1,$$
$$\int_0^1 [s(x) - \bar{s}(x)]\, dx = 0.$$

S(x) – brehmsstrahlung спектър

44

- При малки *x* очакваме морските кварки в протона и неутрона да имат еднакви разпределения.

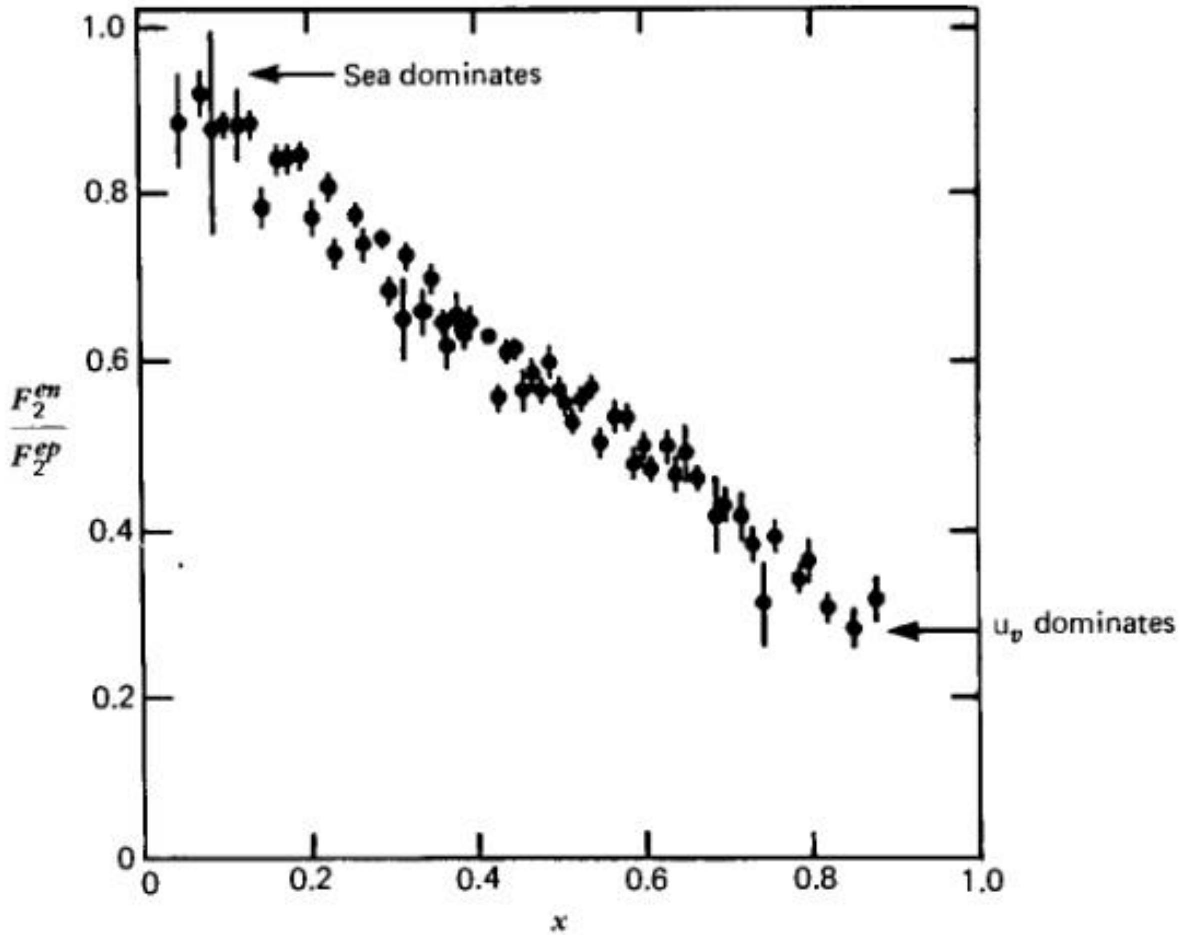

Fig. 9.6 The ratio F_2^{en}/F_2^{ep} as a function of x, measured in deep inelastic scattering. Data are from the Stanford Linear Accelerator.

- Как би трябвало да изглежда $F_2(x)$ според представата, която изградихме за структурата на протона?

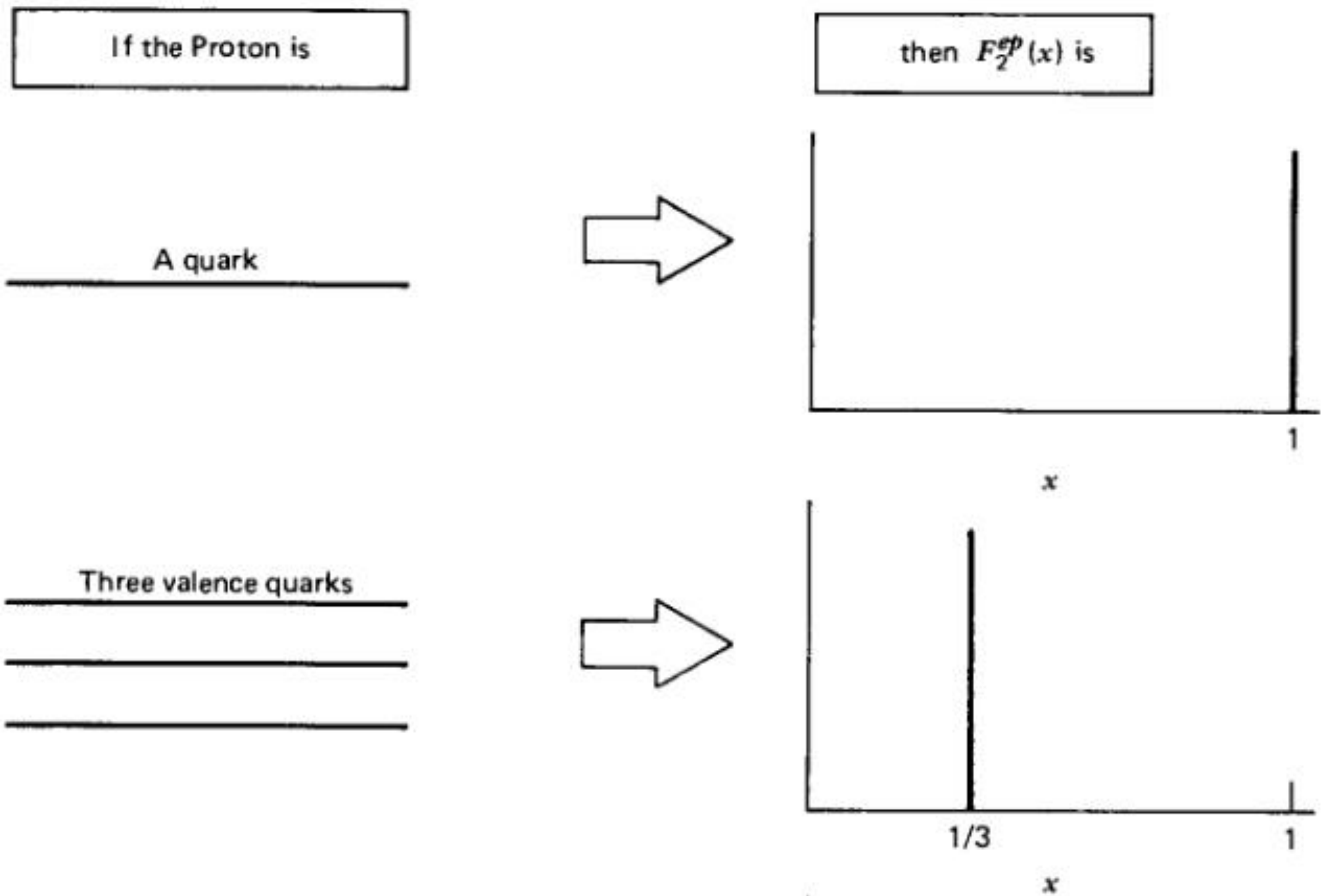

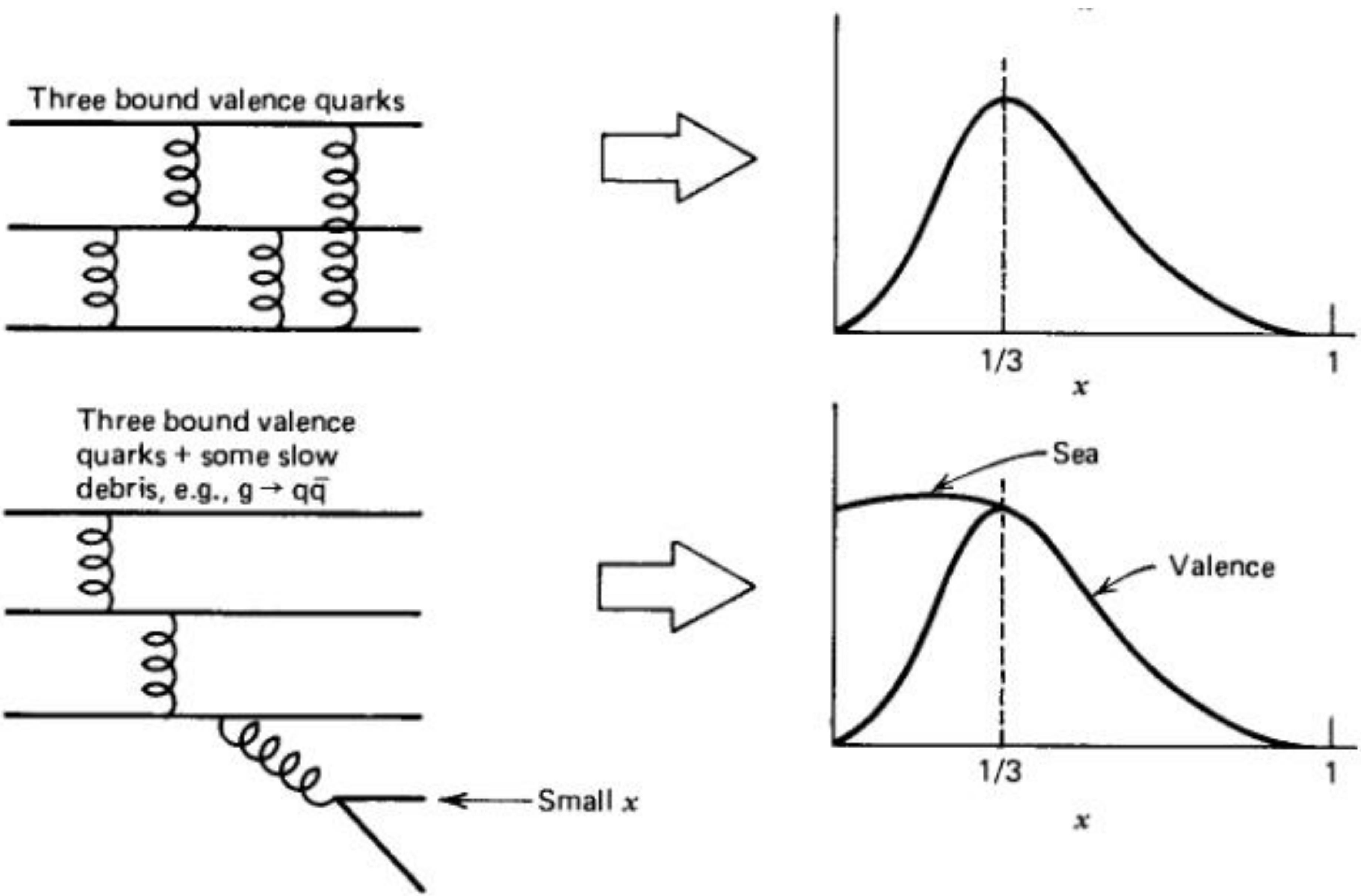
Three bound valence quarks
1/3
1
x
Three bound valence quarks + some slow debris, e.g., g → q$\bar{q}$
Sea
Valence
1/3
1
x
Small x

$$\frac{1}{x}\left[F_2^{ep}(x) - F_2^{en}(x)\right] = \frac{1}{3}\left[u_v(x) - d_v(x)\right]$$

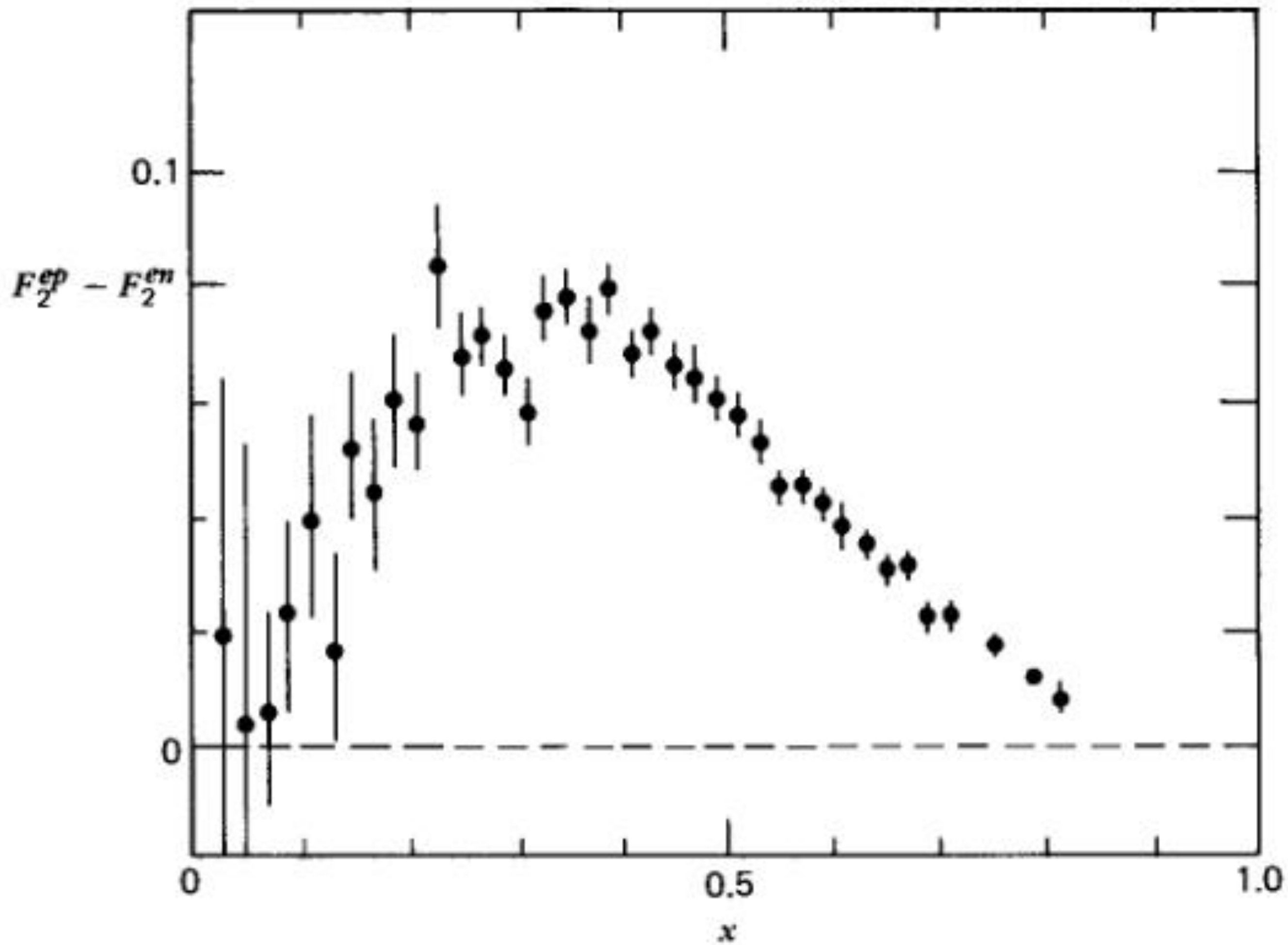

Анализ на експрименталните данни позволява и разделянето на разпределенията по импулси на такива за валентните и морските кварки:

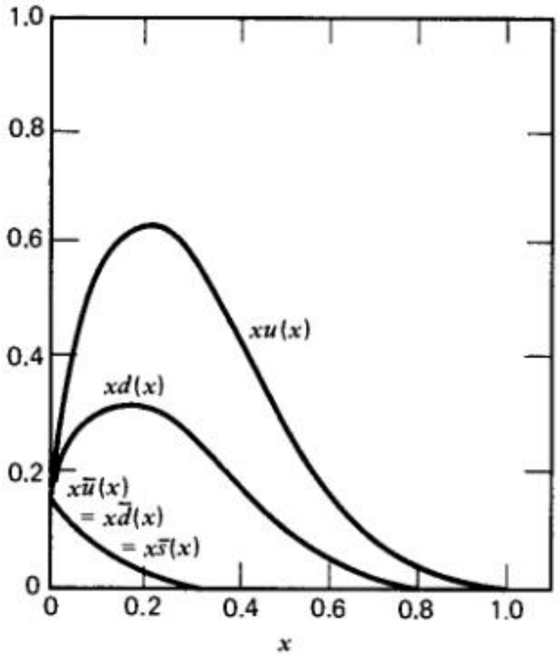

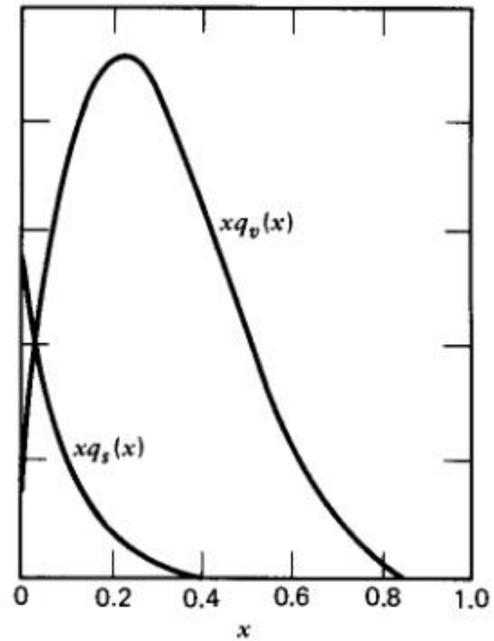

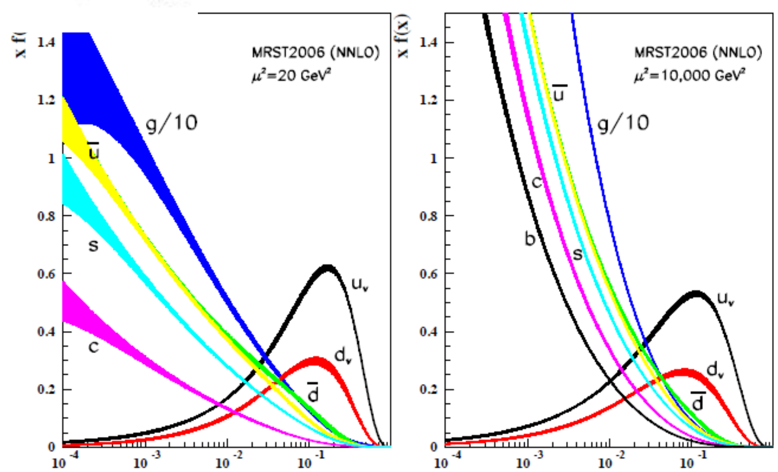

Figure 16.4: Distributions of x times the unpolarized parton distributions $f(x)$ (where $f = u_v, d_v, \overline{u}, \overline{d}, s, c, b, g$) and their associated uncertainties using the NNLO MRST2006 parameterization [13] at a scale $\mu^2 = 20\ \mathrm{GeV}^2$ and $\mu^2 = 10,000\ \mathrm{GeV}^2$.

Ако сумираме приноса от всички кварки трябва да получим пълния импулс на протона. Но с електрони можем да изследваме само разпределението на електричния заряд!

$$\int_0^1 dx\,(xp)[u + \bar{u} + d + \bar{d} + s + \bar{s}] = p - p_g$$

$$\int_0^1 dx\, x(u + \bar{u} + d + \bar{d} + s + \bar{s}) = 1 - \varepsilon_g$$

$$\int dx\, F_2^{ep}(x) = \tfrac{4}{9}\varepsilon_u + \tfrac{1}{9}\varepsilon_d = 0.18,$$

Интегрирането по експерименталните резултати дава следните стойности за приноса в импулса на p и n:

$$\int dx\, F_2^{en}(x) = \tfrac{1}{9}\varepsilon_u + \tfrac{4}{9}\varepsilon_d = 0.12,$$

$$\varepsilon_u \equiv \int_0^1 dx\, x(u + \bar{u})$$

Решаването на тази система дава удивителния резултат че почти половината от импулса на протона се носи от глуоните

$$\varepsilon_u = 0.36, \qquad \varepsilon_d = 0.18, \qquad \varepsilon_g = 0.46$$

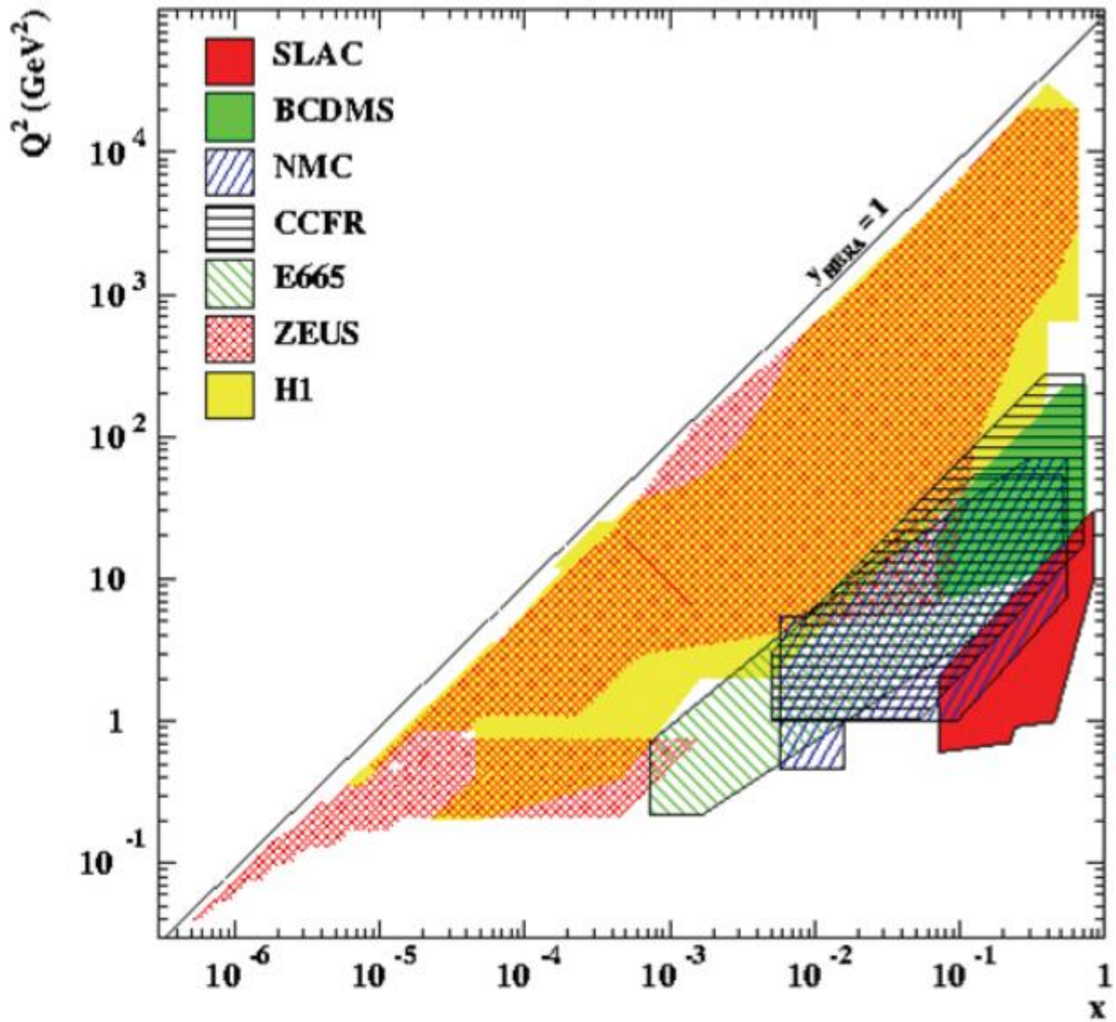

HERA collider :
H1 and ZEUS
1992 – 2007

Fixed target :
SLAC, FNAL and CERN
completed ~10-20 years
ago

DIS at ZEUS

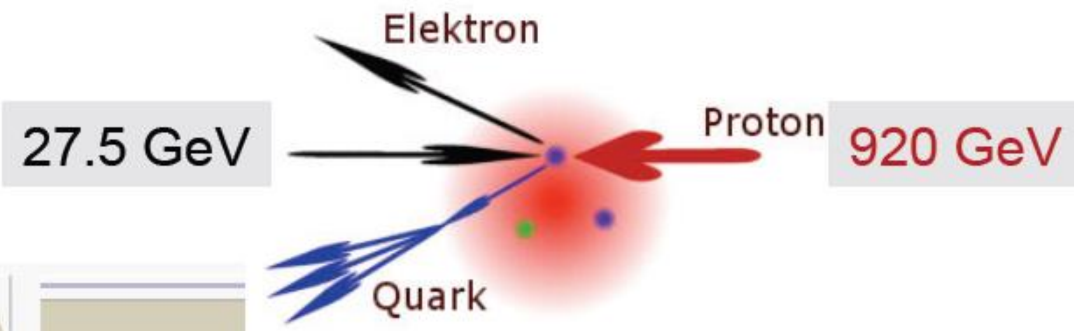

Elektron
27.5 GeV
Proton
920 GeV
Quark

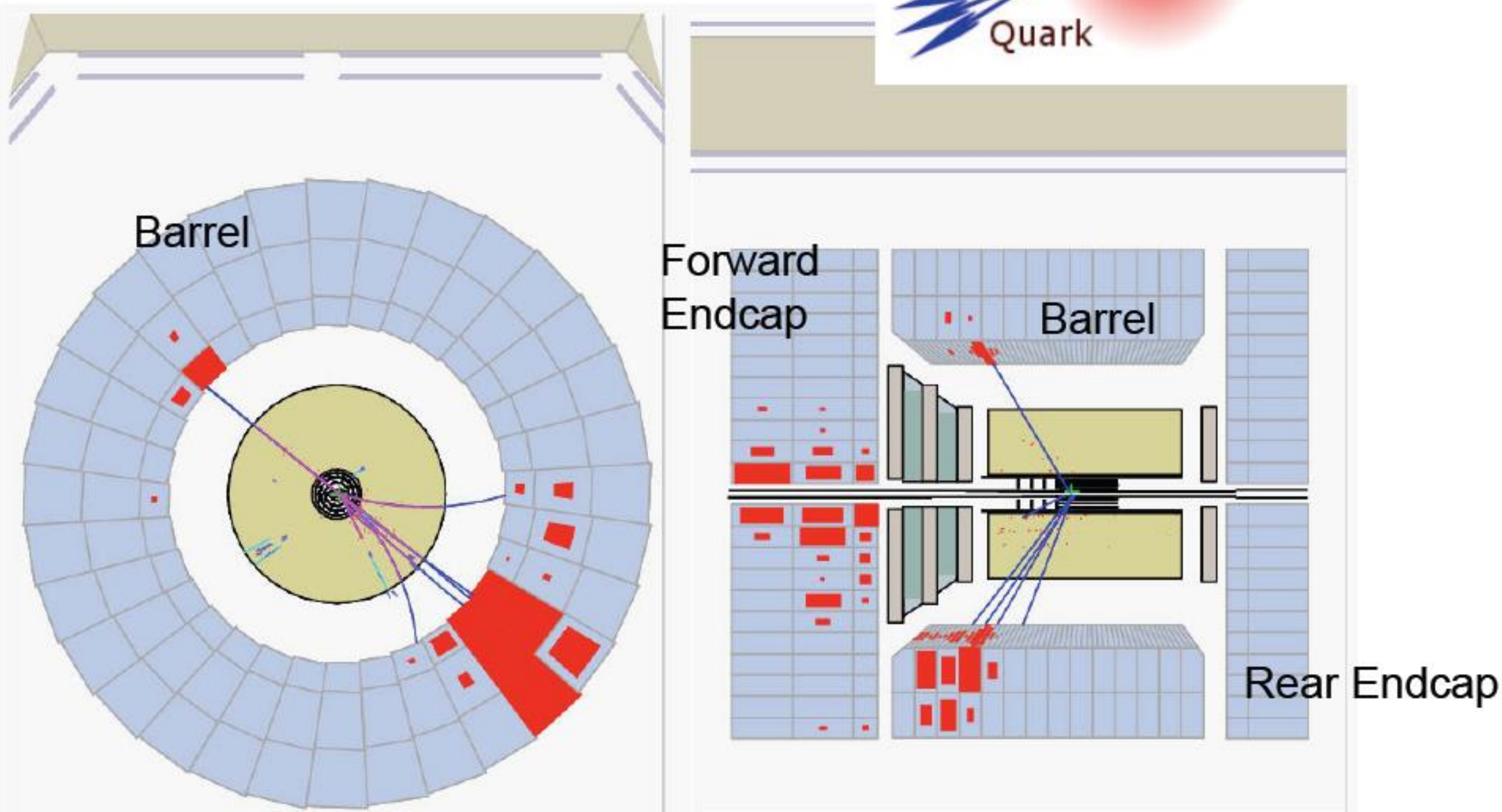

Barrel
Forward
Endcap
Barrel
Rear Endcap

http://pdg.lbl.gov/2011/reviews/rpp2011-rev-structure-functions.pdf

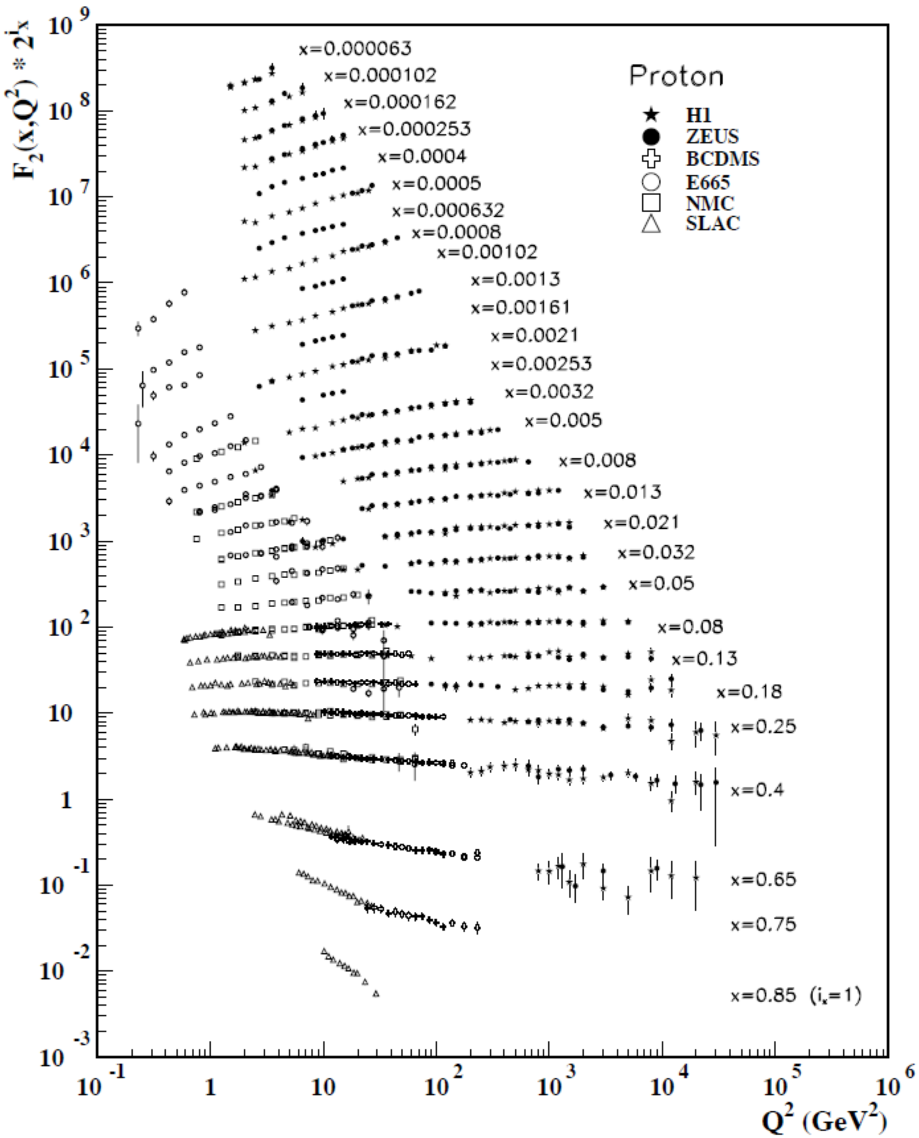

Figure 16.7: The proton structure function F_2^p measured in electromagnetic scattering of positrons on protons (collider experiments ZEUS and H1), in the kinematic domain of the HERA data, for $x > 0.00006$ (*cf.* Fig. 16.10 for data at smaller x and Q^2), and for electrons (SLAC) and muons (BCDMS, E665, NMC) on a fixed target. Statistical and systematic errors added in quadrature are shown. The data are plotted as a

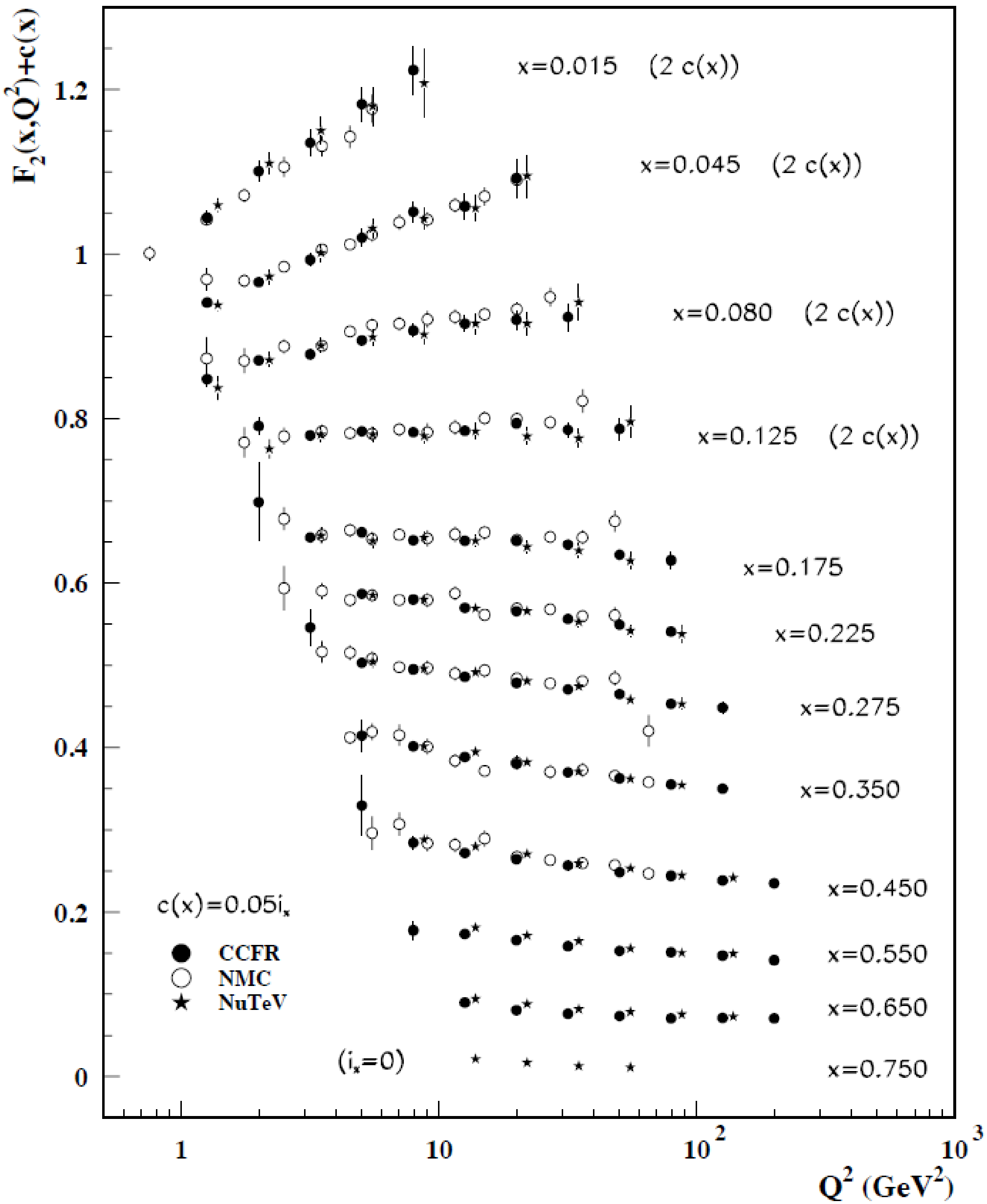

Figure 16.9: The deuteron structure function F_2 measured in deep inelastic scattering of muons on a fixed target (NMC) is compared to the structure function F_2 from neutrino-iron scattering (CCFR and NuTeV) using $F_2^{\mu} = (5/18)F_2^{\nu} - x(s+\overline{s})/6$, where heavy-target effects have been taken into account. The

QCD – F_2 violates Bjorken Scaling $\frac{\partial F_2}{\partial \ln Q^2} \sim \alpha_s x g$

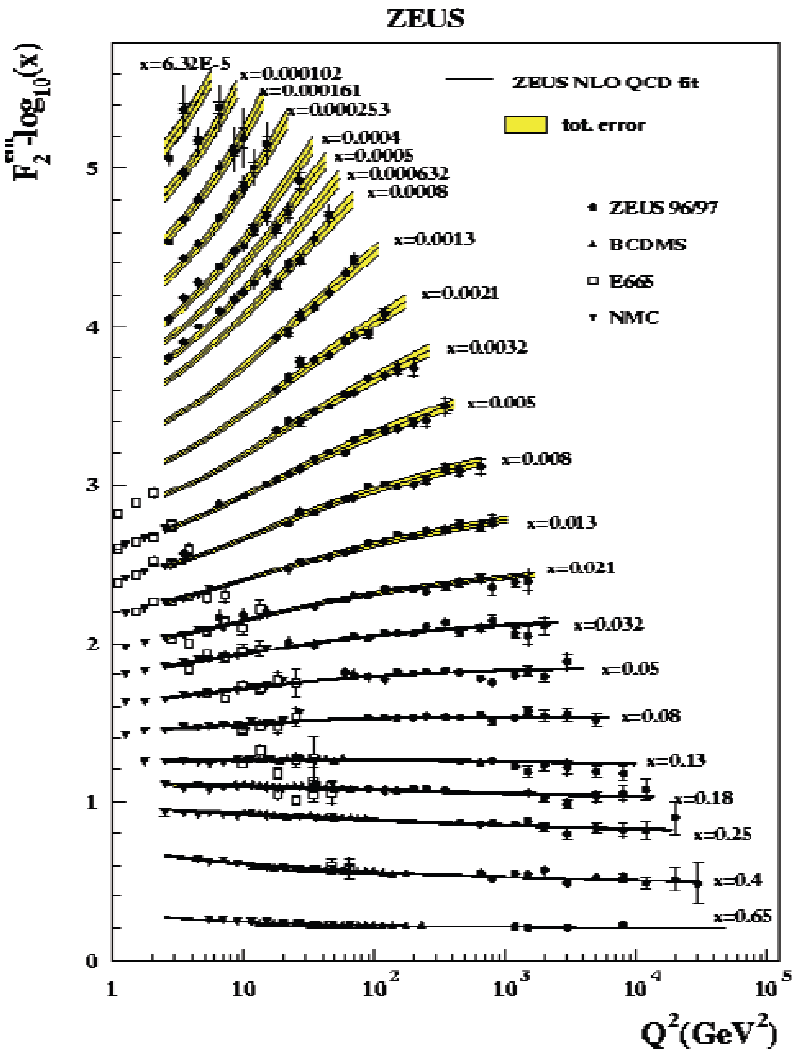

At low x :

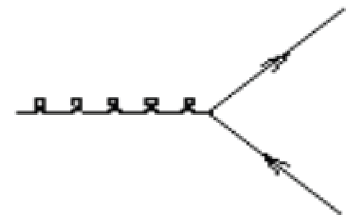

Gluon splitting enhances quark density
➔ F_2 rises with Q^2

At high x :

Gluon radiation shifts quark to lower x
➔ F_2 falls with Q^2

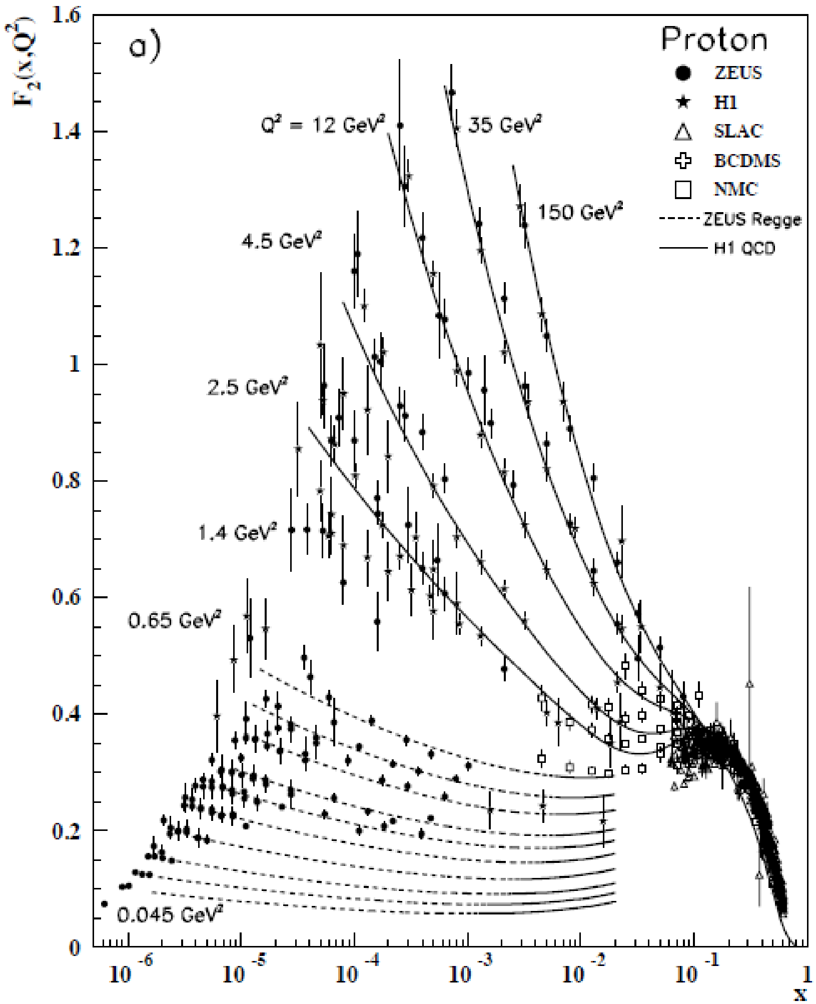

Figure 16.10: a) The proton structure function F_2^p mostly at small x and Q^2, measured in electromagnetic scattering of positrons (H1, ZEUS), electrons (SLAC), and muons (BCDMS, NMC) on protons. Lines are ZEUS and H1 parameterizations for lower (Regge) and higher (QCD) Q^2. The width of the bins can be up to